

**University of Alberta**

Aggregation and Sedimentation of Fine Solids in  
Non-Aqueous Media

by

Maryam Fotovati

A thesis submitted to the Faculty of Graduate Studies and Research  
in partial fulfillment of the requirements for the degree of

Master of Science

in

Chemical Engineering

Department of Chemical and Materials Engineering

© Maryam Fotovati

Spring 2011

Edmonton, Alberta

Permission is hereby granted to the University of Alberta Libraries to reproduce single copies of this thesis and to lend or sell such copies for private, scholarly or scientific research purposes only. Where the thesis is converted to, or otherwise made available in digital form, the University of Alberta will advise potential users of the thesis of these terms.

The author reserves all other publication and other rights in association with the copyright in the thesis and, except as herein before provided, neither the thesis nor any substantial portion thereof may be printed or otherwise reproduced in any material form whatsoever without the author's prior written permission.

## **Abstract**

A major challenge to any “solvent-based” bitumen extraction technology is the removal of suspended fine solids from the hydrocarbon medium (i.e. diluted bitumen). To address this problem, we examined how colloidal solids could be made to aggregate in a hydrocarbon medium and thus be separated by gravity settling. The model solids were micron-sized “bitumen-treated” silica particles; the oil phase was bitumen diluted in an organic solvent of variable aromatic content. On the macroscopic scale, the experiments involved quantifying the settling rates of the particles as the aromatic content of the solvent was varied. Our results showed the existence of an optimal (non-zero) aromatic content at which the solids settling rate was the highest. On the microscopic scale, adhesive forces between individual glass spheres were directly measured using the microcantilever technique (again in non-aqueous media). It was demonstrated that, in addition to being captured by asphaltene networks, the suspended solids could also homo-flocculate — and thus form aggregates and be separated — in an alkane-diluted bitumen environment.

## Table of Contents

1	Introduction.....	1
2	Settling Rate and Inter-Particle Force Measurement.....	9
2.1	Settling Rate.....	10
2.1.1	Sedimentation.....	10
2.1.2	Flocculation.....	12
2.1.3	Effect of Flocculation on Sedimentation.....	13
2.1.4	Settling Rate Measurement Methods .....	13
2.2	Inter-Particle Forces in Colloidal Systems .....	17
2.2.1	Inter-Particle Forces in Liquid Media .....	18
2.2.2	Inter-Particle Forces in Non-aqueous Media .....	21
2.2.3	Inter-Particle Force Measurement Methods .....	24
3	Materials and Methods .....	28
3.1	Macro-Scale Experiments: Settling tests.....	28
3.1.1	Materials.....	28
3.1.2	Sample Preparation for Settling Tests.....	30
3.1.3	Settling Rate Measurement .....	31

3.2	Micro-Scale Experiments: Inter-Particle Force Measurements.....	34
3.2.1	Materials.....	34
3.2.2	Preparation of Micropipette with Rounded Tip .....	36
3.2.3	Making of the Microcantilever.....	38
3.2.4	Force Measurements between Two Glass Spheres by the Microcantilever Technique .....	39
4	Results and Discussion.....	45
4.1	Macro-scale Experiment: Aggregation of Silica Particles in Non- aqueous Media .....	45
4.1.1	Effect of Oil Phase Composition on Solids Settling Rate.....	46
4.1.2	Presence of Bitumen Caused a Delay in the Onset of Sedimentation .....	59
4.2	Micro-scale Experiment: Inter-particle Force Measurements in Non- aqueous Media .....	62
5	Summary and Recommendations .....	68
6	References.....	72

## List of Tables

Table 3.1: Solids and the corresponding hydrocarbon phases that were studied.

..... 34

## List of Figures

Figure 1.1: A very abstract view of the process which separates coarse solids from solvent-diluted bitumen.....	4
Figure 1.2: Schematic of the non-aqueous bitumen extraction process.....	6
Figure 2.1: Sedimentation of concentrated suspensions (a) Type 1 settling, (b) Type 2 settling.....	11
Figure 2.2 : Experimental setup for settling tests measurements through optical method (Long, Dabros, and Hamza 2002, 1945-1952) .....	14
Figure 2.3: Settling curve results (optical method). Segments 1 and 2 represent the positions of the upper and lower interfaces, respectively. Segment 3 represents the interface between consolidation zone and bottom water zone. Point ‘A’ is the merging point of the upper and lower interfaces, which is the point where hindered settling zone disappears and consolidation starts.....	15
Figure 2.4: Macromolecules adsorption on the surface in a) bad solvent (packed structure) b) good solvent (brush-like structure).....	23
Figure 2.5: Polymer cross-bridging between two particles.....	24
Figure 2.6: Schematic of a surface force apparatus (SFA) and its two crossed mica cylinders. ....	25

Figure 2.7: Schematic of an atomic force microscope (left) and an example of colloidal probe (right). The picture shows a glass sphere with a diameter of approximately 10  $\mu\text{m}$  that is glued to the end of a triangular AFM cantilever..... 26

Figure 3.1: Sample preparation procedure ..... 31

Figure 3.2 : Schematic of the sedimentation experiment. (a) Samples were taken from a fixed location — in this case, 1 cm from the free surface. The amount of solids in each sample was denoted  $m$ , and the settling time denoted  $t$ . (b) Typical plot of  $m$  versus  $t$ . The initial slope  $dm/dt$  was chosen as a measure of the settling rate. .... 33

Figure 3.3: Rounded tip of a micropipette ..... 36

Figure 3.4: Pipette puller apparatus. The magnified picture shows the glass capillary tube (OD: 1 mm and ID: 0.7 mm) positioned in the middle of a platinum wire ready to be stretched at high temperature. .... 37

Figure 3.5: The ‘micro-forging’ apparatus (platinum hot wires shown on the right)..... 37

Figure 3.6: A sketch of the micro-cantilever. The magnified views are actual microscope images taken with a 40 $\times$  objective lens. The diameter of the tip is roughly 30  $\mu\text{m}$ . .... 38

Figure 3.7: A schematic of the micro-cantilever setup. A hydrocarbon solvent was first placed in a small holding cell (also shown in the magnified view). Two

micropipettes were then inserted into this environment: a straight pipette from the left, and a micro-cantilever from the right. As seen on the monitor (an actual photograph), both pipette tips had rounded shapes and could function effectively as spherical particles. .... 39

Figure 3.8: (a) A sketch of the microcantilever experiment for determining the adhesive force between two pipette tips (functioning as glass particles). The cantilever on the right was kept stationary throughout the experiment. (b) Actual microscope images of a force-measuring experiment. When the pipette on the left was pulled back, the adhesive force between the tips caused the cantilever to be deflected from its original position by an amount  $\delta$ . The cantilever deflection provides a direct measure of the adhesive force. .... 43

Figure 4.1: Effect of solvent aromatic content on the settling rate of silica particles in heptol (a mixture of toluene and *n*-heptane). There was no dissolved bitumen in the oil phase. .... 47

Figure 4.2: Bitumen-coated solid particles in (a) a paraffinic solvent, (b) an aromatic solvent. .... 49

Figure 4.3: Microscope images of bitumen-treated silica in mixtures of toluene and *n*-heptane at various ratios: (a) 100% toluene, (b) equal volumes of toluene and heptane, (c) 100% heptane. .... 50

Figure 4.4: Effect of bitumen concentration on the settling rate of bitumen-treated silica. The suspending liquid was heptol-diluted bitumen solution. .... 53



Figure 4.5: Schematic of aggregates formed by (a) single particle addition, and (b) cluster-cluster aggregation. .... 57

Figure 4.6: Hypothetical schematic of asphaltene floc shapes in heptane-rich heptol. The floc shapes at 20 vol% heptol (i.e. 8 parts heptane + 2 parts toluene by volume) is more spherical and denser than those at higher heptane contents. 58

Figure 4.7: Experimental silica particles settling curves for a system (a) without bitumen and (b) with bitumen. In case (a) settling began immediately after mixing was stopped, whereas case (b) shows a *delay time* for particles to begin sedimentation. .... 59

Figure 4.8: Effect of bitumen concentration on the delay time (delay time was illustrated in Fig. 4.7b). Note that the delay time vanished when (i) there was no bitumen in the oil phase, and (ii) the toluene content in heptol was 30 vol% of greater. .... 61

Figure 4.9: Adhesive force between two bitumen-treated glass spheres in heptol-diluted maltene ('maltene' = de-asphalted bitumen). The amount of maltene in solution was approximately 2 wt%. .... 65

## Nomenclature

$m$	Mass	(kg)
$t$	Time	(s)
$Q$	Magnitude of electric charge	(C)
$D$	Separation distance	(m)
$R$	Radius	(m)
$A$	Hamakar constant	(J)
$V_s$	Particle settling velocity	(m/s)
$d$	Hydrodynamic diameter	(m)
$g$	Gravitational acceleration	(m/s <sup>2</sup> )
$l$	Length of centrifugal tube	(m)
$K_b$	Micro-cantilever stiffness	(N/m)
$F$	Force	(N)
$\rho_p$	Density of particles	(kg/m <sup>3</sup> )
$\rho_f$	Density of fluid	(kg/m <sup>3</sup> )
$\mu$	Fluid viscosity	(Pa.s)
$\delta$	Micro-cantilever deflection	(m)

## **1 Introduction**

The Canadian oil sands, with 173 billion barrels of proven oil reserves, is one of the largest petroleum resources in the world (Anonymous 2004, 22-23). The oil sands in Alberta accounts for more than 90% of Canada's total oil reserves. In a broader view, in terms of proved reserves, Canada holds the second place just after Saudi Arabia (with a reserve of 260 billion barrels). At present, production of more than one million barrels of high-grade synthetic crude oil per day has already made this country the largest foreign oil supplier for the United States; roughly 21% of US total crude oil import is provided by Canada. According to the National Energy Board of Canada, this current rate of oil production is expected to triple by year 2015 (Board NE 2006).

Currently, commercial recovery method of bitumen from oil sands is classified as 'water-based extraction': mined oil sand ores are first crushed and slurried in warm water; mechanical energy in the form of agitation or pipeline transport is introduced into the slurry to promote detachment of bitumen from sand grains; conditioning process with the aid of several additives also helps the bitumen to be liberated from the sand grain surfaces. The mixture is then pumped into large water-filled vessels (called the primary separation vessel) to accomplish bitumen separation through a flotation process. The product, in the form of a "froth" (overflow of the separation vessel), typically consists of 60 wt% bitumen, 30 wt% water, and 10 wt% solids (Xu, Dabros, and Hamza 2007, 413-418). This froth

must be further treated — in a process called “froth treatment” — to remove the unwanted water and solids from the froth. After froth treatment, the bitumen content is typically more than 99% by weight.

Along with the clear economic benefits, there are also serious environmental issues associated with the ‘water-based’ bitumen extraction method. The main issues are environmental in nature; they are caused by oil losses through the reject solids and also consumption of excessive amounts of water and energy as required by the water-based extraction process. Therefore, despite the economical benefits of the oil sands industry, its environmental impacts are not ignorable. Here, our particular concern is the consumption of large volumes of water by the current water-based process. Fresh water is required throughout the plant for different purposes such as utility functions and separation of bitumen from sand. This excessive water consumption can result in the following environmental problems (Woynilowicz, Severson-Baker, and Reynolds 2005):

- The Athabasca River — the main source of water for the current oil sands operations — also supplies fresh water to the city of Fort McMurray, its neighbouring communities and the Lake Athabasca extended deltas. Current rate of water consumption has negative impact on these communities and ecosystems. Large amounts of water withdrawal from the river (especially in low flow months) and changes in water quality will endanger the aquatic life in the Athabasca River. For instance, there is already reported damage to the habitat of many

fish species. (Approved oil sands projects are licensed to withdraw 349 million m<sup>3</sup> of fresh water per year from the Athabasca River. This amount of water is roughly the water usage by a city twice the size of Edmonton (Woynillowicz, Severson-Baker, and Reynolds 2005).

- The first and unavoidable step in ‘water based’ bitumen extraction is making bitumen slurries from mined oil sands. As water is known to have one of the highest heat capacities among condensed materials, bitumen extraction requires enormous amounts of thermal energy to heat the water (up to 80°C). This in turn increases demands on natural gas consumption, leading to its eventual depletion. The issues of greenhouse gas emissions is another obvious environmental issue.
- By law, water that is contaminated by the bitumen extraction process cannot be released back to the environment. This water must therefore be kept “temporarily” in large tailings ponds. These tailings ponds can cause several environmental issues, such as contamination of surface water and surrounding soils through leakage of contaminants from the ponds.

With anticipated expansion in oil sands production due to ever-increasing global oil demand, the above-mentioned problems — which stem from excessive water usage — have progressed to a point where the future of the oil sands industry may be in jeopardy. In view of these issues, development of an alternative *solvent-based* (or *non-aqueous*) extraction technology appears to be necessary. The basic principles of such a non-aqueous technology are simple.

Mined oil sands are first mixed with an organic solvent in which bitumen is soluble. The mixture is then fed into coarse solids separation vessels in which the separation can be achieved via traditional methods — such as centrifugation, filtration, or other means (see Figure 1.1). The rejected solids leave the separation vessel from the bottom, while the overflow, which contains diluted bitumen, forms the product stream. The solvent in the product stream can be recovered through a distillation process and be reused upstream (for mixing with mined oil sands). The extracted bitumen is sent downstream for further upgrading into synthetic crude oil.

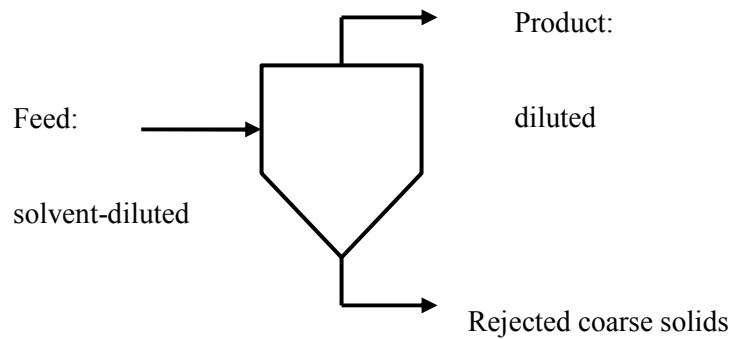


Figure 1.1: A very abstract view of the process which separates coarse solids from solvent-diluted bitumen.

In the past several decades, many non-aqueous processes had been proposed for bitumen extraction (Long, Dabros, and Hamza 2002, 1945-1952)(Sparks and Meadus 1981, 251-264)(Farnand, Meadus, and Sparks 1985, 131-144). Unfortunately, none of these methods had progressed beyond pilot stages. The

two common obstacles in all proposed non-aqueous processes, causing their failure, are:

1. Failure to remove fine solids (e.g. clays, asphaltenic aggregates, etc.) from the oil phase (i.e. diluted bitumen) will result in fouling of catalysts and pipelines in general.
2. Failure to recover the residual oil trapped in the reject sand grains will result in solvent loss, and eventually pollution of the environment on a very large scale.

To develop a successful solvent-based extraction process, the mechanisms which underlie the above two obstacles must be understood before any commercialization plan is attempted.

This M.Sc. research is motivated by the first obstacle mentioned above, namely, the removal of unwanted fine solids from a diluted bitumen medium. Figure 1.2 shows where this issue exactly occurs in the solvent-based bitumen extraction process. The majority of fine particulates are ultrafine clays and silica particles with sizes ranging from 10 nm to 10  $\mu\text{m}$ . It is important to note that conventional methods of separation (e.g. centrifugation or filtration) are only able to remove particles larger than about 100 microns. It means that these usual methods of separation are not practical for eliminating fine particulates (under 100  $\mu\text{m}$ ). However, if we could identify suitable conditions under which fine particulates can be destabilized in suspensions, it could result in their aggregation

(i.e. forming big clusters of fine solids). It would then be possible to remove the aggregates using conventional separation methods such as gravity settling.

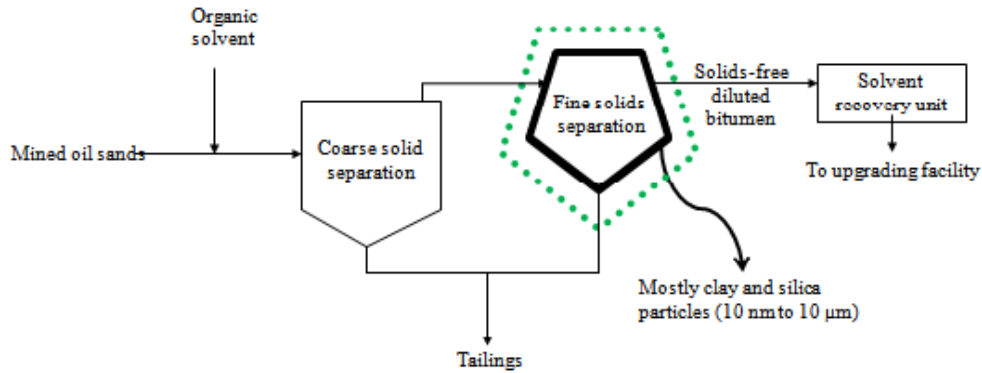


Figure 1.2: Schematic of the non-aqueous bitumen extraction process.

Recently, it was discovered serendipitously that using a paraffinic solvent as diluent during froth treatment can result in the aggregation of all suspended fine solids, which leads in turn to their complete removal by simple gravity settling. This is the so-called paraffinic froth treatment (PFT) process. Many studies have been conducted on this new process (Long, Dabros, and Hamza 2002, 1945-1952)(Chia and Yeung 2004, 619-621). The PFT process is beginning to be implemented by several oil sands operators (e.g. Albian Sands) and could produce a diluted bitumen product that is free of water (Romanova et al. 2004, 710-721). To a certain degree, this PFT process is similar to what one would expect to see during solvent-based extraction. The mechanism behind this PFT process, however, is also still not understood. It is not clear, for example, if the “floc networks” which result from asphaltene aggregation are responsible for entrapping and collecting all water droplets and fine solids in the hydrocarbon



medium. In the absence of emulsified water, is the PFT process capable of aggregating and removing suspended fine solids, or is water essential as a “collector” of the largely hydrophilic fine solids? In this thesis, it is our goal to uncover the fundamental mechanism(s) behind sedimentation of solid particles, resulting in their elimination, in non-aqueous suspensions (i.e. diluted bitumen). The following are our objectives in this study:

1) *On the macroscopic scale*: To systematically examine the sedimentation of silica particles (used here as our model inorganic solids) in various hydrocarbon media. The hydrocarbon media are mixtures of toluene and heptane at different ratios (to allow for different degrees of “aromatic content” in the solvent); bitumen may also be added to these toluene-heptane mixtures. This system is simplified by design such that it does not contain any emulsified water (the presence of water may complicate the understanding of solids aggregation in hydrocarbon). All silica surfaces in this study were first “bitumen-treated,” i.e. they had been pre-exposed to bitumen so that the surface properties of silica could be altered through adsorption of bitumen species.

2) *On the microscopic scale*: The forces between individual silica particles were studied using a novel *microcantilever technique*. These interparticle forces are important as they ultimately dictate the colloidal stability of solids suspensions on the macroscopic scale.

The focus of this research will be on the underlying mechanism behind the aggregation and removal of fine particles that are dispersed in an oil medium.

This has obvious relevance to the non-aqueous extraction of bitumen, as the success of this technology depends critically on the removal of fine solids from a diluted bitumen environment. This study will provide insight into the adhesive forces which act between microscopic particles in hydrocarbon solvents, and also the mechanism behind the PFT process. This thesis is organized into the following chapters:

Chapter 2 will provide background information on the basics of sedimentation process and the techniques of settling rate measurement. Also, inter-particle forces in colloidal systems and their measurement methods, both in macro- and micro-scales, are discussed. Chapter 3 covers two experimental approaches that are used to study the underlying physics of particles aggregation and their forces. In the first approach, macro-scale experiments are conducted to determine the settling rate of silica particles in organic solvents with different degrees of aromaticity (i.e. different proportions of toluene). Also, the relation between particle settling rate and bitumen content in suspension is studied. In the second approach, a novel micro-scale technique, called the *micro-cantilever*, was developed for this study to measure adhesive forces between silica particles. The experimental results and discussion on the underlying free settling mechanisms in non-aqueous media are provided in Chapter 4. Finally, the contributions of this research and suggestions for future work are discussed in Chapter 5.

## 2 Settling Rate and Inter-Particle Force Measurement

As mentioned in Chapter 1, the main challenge to solvent-based bitumen extraction is the removal of suspended fine solids in the oil phase (i.e. diluted bitumen); this is to avoid further problems in the upgrading facilities, such as the fouling of catalysts. In separation processes, both the material and size are important. To be more specific, these solid particles are mainly quartz grains which consist ~95% of Athabasca oil sands mineralogy (Mossop 1980, 145-152). Quartz is made up of  $\text{SiO}_2$ , and it is hydrophilic in nature and normally does not strongly associate with bitumen. For coarse sands, conventional separation methods (e.g. filtration or centrifugation) are applicable. However, a considerable amount of quartz particles found in bitumen froth are fine particles which are not easy to separate. These ultra-fine particles, with major dimensions of  $< 0.3 \mu\text{m}$ , can adversely affect the separation process and quality of bitumen through complex interactions with components of the oil phase.

To improve the separations technology, study of the mechanisms behind flocculation and sedimentation of fine particles in non-aqueous (i.e. organic) liquids seems necessary. Thus, the basic concepts of settling and sedimentation, along with fine particles interactions (with one another and with bitumen components) will be discussed in this chapter.

## 2.1 Settling Rate

### 2.1.1 Sedimentation

Suppose an isolated particle is moving through a fluid in a gravitational field. It rapidly reaches its terminal settling velocity when all the forces acting on it (i.e. frictional and gravitational forces) come to balance. However, in a real process, we are dealing with suspensions of particles at high concentrations — not just one isolated particle. In a highly concentrated suspension, significant interaction between particles will occur, and more effective frictional forces will be exerted on them, which will hinder the settling of particles (Oliver 1961, 230-242). As a consequence, in comparison with particle sedimentation under *free settling* conditions (with little or no mutual interference amongst particles), the sedimentation rate of a particle in a concentrated suspension would be significantly less.

A study by Coe and Clevenger showed that particles in concentrated suspensions may settle in one of two ways (Coe and Clevenger 1916), as shown in Figure 2.1. Figure 2.1a illustrates a stage in “Type 1 settling,” which occurs more commonly in practice. At first, agglomeration of fine solids results in a brief accelerated settling of the suspension, followed by creation of a *clear liquid* zone on the top (section A). Then, the interface between the clear liquid and the rest of the suspension moves downward in a more-or-less constant rate. In this zone (section B), which is called *hindered or settling* zone, particles with a strong tendency to coalesce do so and settle as a unit (or *floc*), with individual particles remaining in fixed positions relative to each other within the floc. All of the

particles within the matrix settle at the same velocity. In the meantime, bigger particles accumulate at the bottom of the jar and form a *sediment layer* (section D). As settling proceeds, zone B shrinks until the moment it completely disappears, and the upper interface (between sections A and B) reaches the lower interface (between sections B and D). At this point, a direct interface is formed between *clear liquid* and *sediment layer*.

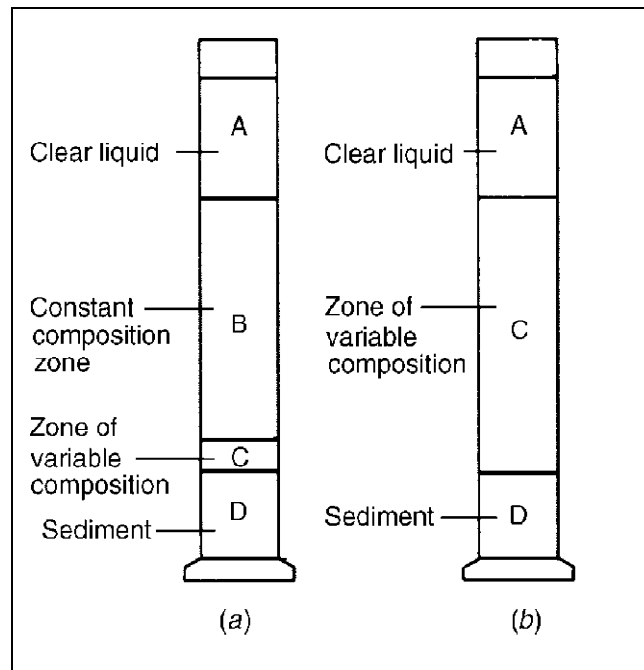


Figure 2.1: Sedimentation of concentrated suspensions (a) Type 1 settling, (b) Type 2 settling.

Later on, anymore sedimentation results from consolidation of the sediment layer at the bottom which occurs under compression settling regime. The compressive forces resulted from the weight of suspension column on the top of sediment layer, forcing the liquid (in sediment layer) upward and then form a loose bed of particles (section C) (Richardson, Harker, and Backhurst 2002). The

second and rather less common type of sedimentation in concentrated suspensions is shown in Figure 2.1b. This is the more likely type of sedimentation when the particle size range is very large. In this case, bigger particles settle faster and leave the smaller ones behind, resulting in the formation of a zone of *variable composition* (section C). The sedimentation rate progressively decreases during the whole process.

Generally, it is very difficult to characterize the sedimentation rate of a suspension of fine particles due to the large number of factors affecting the process. Although a number of empirical equations are available for this purpose, they mostly are limited to some specific conditions and the range of their applicability is very narrow.

### **2.1.2 Flocculation**

The flocculation of fine particle affects the suspensions stability considerably. In general, flocculation occurs when primary particles come together and creates large conglomerations (Richardson, Harker, and Backhurst 2002). The density of these conglomerations, which usually appear as loose structures, happens to be between that of the constituent particles and the trapped liquid. Then, if there is sufficient density difference between the aggregate and the suspending liquid, it could be separated from the suspension by sedimentation. The tendency of colloidal particles in suspension to aggregate and form heavier flocs has always been of interest to the industries due to its wide application in solid-liquid separation processes (e.g. sedimentation, filtration and waste water treatment).

Aggregation between colloidal particles has its origin in inter-particle forces. Particles in a liquid suspension collide due to their Brownian motions or hydrodynamic trajectories. As the particles come into close contact during collision, they can feel attractive and/or repulsive forces that are between the solids. Depending on the liquid media, these forces may react in different ways. The main effective forces in colloidal suspensions are van der Waals attraction and electrostatic repulsion, which are due to different mechanisms. More discussion on the different types of inter-particle forces and their behaviours would be given in section 2.2.

### **2.1.3 Effect of Flocculation on Sedimentation**

Gravity sedimentation is the simplest and cheapest form of separation process. Here, the settling rates of aggregates and sediment volumes is a strong function of the volumetric concentration of flocs and the inter-particle forces. As a result, whenever flocculation is the main cause of sedimentation, the settling behaviour of suspensions depends largely on the initial solid concentration and chemical environment. Knowing this fact, controlling these two factors can result in identification of optimal settling rate for different suspensions.

### **2.1.4 Settling Rate Measurement Methods**

#### **2.1.4.1 Optical Method**

In this method to measure the settling rates of particles (more precisely, aggregates) optical characteristics have been applied. This is the most common

method of settling rate measurement, which is based on following the interface. A schematic of the experimental setup can be seen in Figure 2.2. The procedure is as follows.

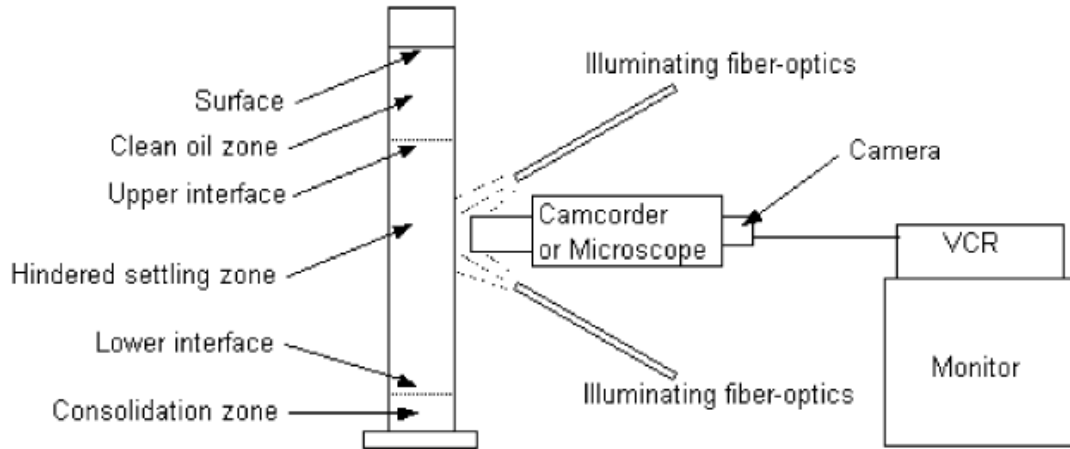


Figure 2.2 : Experimental setup for settling tests measurements through optical method (Long, Dabros, and Hamza 2002, 1945-1952)

Upon completion of mixing, the solution is quickly transferred to a graduated glass cylinder. The observed area of settling is illuminated by two fibre-optic cables. The position of interfaces in the settler varies with time and these movements are recorded with a camcorder or light microscope coupled with a camera and a VCR. After analyzing the recorded movies, the settling chart, which simply is the positions of the interfaces versus time, will be plotted. Here, the settling rate is defined as the descending velocity of the upper interface. To measure the velocity, the slope of a linear line fitted to the initial part of the upper interface curve should be calculated (Zahabi et al. 2010, 3616-3623). In the typical settling rate graph shown in Figure 2.3 (Long, Dabros, and Hamza 2002,



1945-1952), the red line, which is the fitted linear line, is the representative of settling rate in this method.

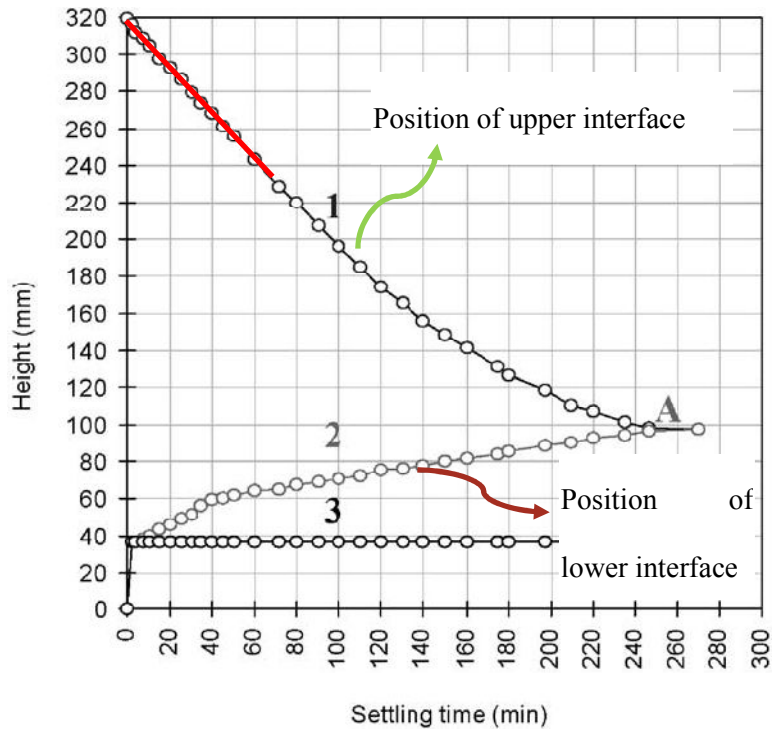


Figure 2.3: Settling curve results (optical method). Segments 1 and 2 represent the positions of the upper and lower interfaces, respectively. Segment 3 represents the interface between consolidation zone and bottom water zone. Point 'A' is the merging point of the upper and lower interfaces, which is the point where hindered settling zone disappears and consolidation starts.

Although this method appears to be perfect and precise for measuring the sedimentation rate in solid-liquid suspensions, visibility is a limiting factor. Application of this method is only limited to solutions which are sufficiently transparent. If the suspending liquid is very opaque (e.g. crude oil), the motion of the interface cannot be followed easily, and the method becomes ineffective.

Another important consideration is that the optical method only works well if the interface between the clear liquid and the dispersed solids remains sharp throughout. In practice, this interface often becomes more dispersed (i.e. blurred) as settling progresses. For the present research, we encounter both problems: the suspending liquid (diluted bitumen) can be very opaque, and the interface between the supernatant and solids suspension tends to become very diffuse. As such, we must think of another approach of characterizing sedimentation rates.

#### **2.1.4.2 Novel Ashing Technique**

When it comes to very dark suspending liquids, the deficiency of the optical method for measuring settling rates compels us to develop an alternative technique. In what follows, a novel *ashing* method is introduced which is capable of measuring the settling rate even in dark liquids. In this method, instead of following the interface, the solids concentration at a *fixed* location in the settling vessel is tracked over time. To do so, upon completion of mixing and transferring the suspension to the settler, sedimentation is allowed to commence (at time  $t = 0$ ). During settling, small samples of suspension are withdrawn from the vessel at different times, and always from the *same* location (usually at a depth of 1 cm from the free surface); each withdrawn sample (typically 0.5 mL) is then analyzed for solids content by “ashing” (i.e. by burning away all aqueous and organic contents and leaving behind only the inorganic “ash”). Ash content is analyzed using a furnace suitable for ashing process according to a standard ASTM

method. A plot of the mass  $m$  of the residual solids (at a fixed location) versus time  $t$  — which we will call the  $m$  vs  $t$  plot from here on — can provide useful information on the sedimentation process. The slope of the initial part of the  $m$  vs  $t$  plot can be used as a representative measure of the settling rate. A more detailed description of the ashing method will be given in Chapter 3. For a schematic diagram of this method, see Figure 3.2.

## **2.2 Inter-Particle Forces in Colloidal Systems**

For a solids suspension, colloidal stability depends on the interaction of the various attractive and repulsive forces acting between the particles. Thus, if repulsive forces are dominant, it means the colloidal particles will be stable in dispersion. The attractive forces are similar in all suspensions; however, the repulsive forces may be electrostatic or steric in nature (Homola and Robertson 1976, 286-297). The type of forces often observed in colloidal systems are short ranged, meaning they can only act if the particles are practically in contact with one another (separated by distances of at most  $\sim 10$  nm). Compared to covalent or hydrogen bonds, colloidal forces are considered relatively weak forces, but they can have a major effect on collision efficiencies and on the adhesion between particles (Gregory 1993, 1-17). A more detailed description of the different kinds of colloidal forces will be discussed in following.

## 2.2.1 Inter-Particle Forces in Liquid Media

### 2.2.1.1 Coulombic Interaction

Originated from electrostatic interaction, Coulombic interactions occur between two charged particles. As two like charges are brought together, they will repel each other; unlike charges, on the other hand, will attract. The Coulombic force  $F$  between two charged particles separated by a distance  $D$  is (Butt, Graf, and Kappl 2003)

$$F \propto \frac{Q_1 Q_2}{D^2}$$

where  $Q_1$  and  $Q_2$  are the magnitudes of the two charges (in coulombs).

### 2.2.1.2 Van der Waals Attraction

The van der Waals force is a universal inter-molecular force, and typically is attractive. It has been considered to consist of three different types of dipole-dipole interactions: Keesom orientation forces (permanent dipole-permanent dipole interactions), Debye induction forces (permanent dipole-induced dipole), and London dispersion forces (induced dipole-induced dipole interactions). Thus, the total van der Waals force is equal to the summation of these three terms. *On average*, the van der Waals (VDW) interaction is *always attractive*, and the potential energy of interaction  $E$  between two molecules varies as  $E \sim 1/D^6$ , where  $D$  is the separation distance between the two point entities.

When it comes to macroscopic objects, the attractive van der Waals force results from the complex interactions between the molecules of those two objects

and the separating environment. The attraction between macroscopic particles depends on the particles size, the distance between them, and the composition of the particles. For instance, the VDW interaction between two spherical particles of radii  $r_1$  and  $r_2$ , in the case that the inter-particle distance at closest approach  $D$  is much less than  $r_1$  and  $r_2$ , is given by (Israelachvili 1992)

$$V_{VDW} = -\frac{A r_1 r_2}{6D(r_1 + r_2)} \quad (2.1)$$

where  $A$  is the Hamakar constant (which relates to the materials of the interacting bodies *and* the medium). If the two spheres are made of different molecules 1 and 2, equation (2.1) remains the same but the Hamaker constant becomes  $A_{12}$  as follows:

$$A_{12} = \sqrt{A_{11} A_{22}}$$

Further, when the two spheres are submerged in a third substance, the Hamaker constant for the interaction of sphere 1 with sphere 2 across the medium 3 is given by

$$A_{132} = \left( \sqrt{A_{11}} - \sqrt{A_{33}} \right) \left( \sqrt{A_{22}} - \sqrt{A_{33}} \right)$$

### 2.2.1.3 Electric Double Layer Repulsion

When a particle is placed in a polar medium (e.g. an electrolyte), it often acquires a surface electric charge. If the suspending medium were an electrolyte, the charged surface will attract ions of the opposite sign via Coulombic forces. The ions that adsorbed onto the immediate surface of the particle is rather

immobile; it is the so-called Stern layer, and has a thickness of typically a few ionic radii. The second layer comprises of counter ions which form a loose, cloud-like structure around the charged particle. This second layer, often called the diffuse layer, is composed of free oppositely-charged ions that move about in the fluid under the influence of electrical attraction and thermal motion. Unlike in the case of the Stern layer, counter ions in the diffuse layer are not firmly anchored to the surface. Considering the Stern and diffuse layers around the particle, the whole region near the surface of enhanced counter-ion concentration is called the electrical double layer (EDL). The concentration of counter-ions drops off exponentially with increasing distance from the surface. The characteristic length of this exponential decay is called the *Debye length* ( $1/\kappa$ ); where  $\kappa$  increases as the square root of the ion concentration. When two charged surfaces are close enough such that the separation distance is of order  $1/\kappa$ , the concentration of counter-ions in the gap will be higher than that in the bulk. This will give rise to an *osmotic pressure* in the gap, which acts to push the two surfaces apart. This is the origin of the electric double layer (EDL) repulsion.

#### **2.2.1.4 Combined Interactions**

According to the DLVO theory, the interaction energy between two colloidal particles could be due to one of the following:

- a) A repulsive interaction  $V_R$  due to overlap of the electrical double layers
- b) An attractive interaction  $V_A$  due to van der Waals forces

The overall or total interaction energy  $V_T$  is additive, i.e.

$$V_T = V_R + V_A$$

While  $V_R$  helps to keep the particles dispersed in solution,  $V_A$  acts to destabilize the dispersion through coagulation. The final condition of the suspension depends on the interplay between these two types of forces.

### **2.2.2 Inter-Particle Forces in Non-aqueous Media**

In non-aqueous media, the colloidal forces are quite different from those in aqueous media. The electric double layer repulsion could occur in a colloidal dispersion only if the surrounding medium is aqueous or polar, i.e. it must be able to solubilize free ions and allow for their transport toward oppositely-charged surfaces. However, in a non-polar environment (such as toluene and heptane in this study), the very low solubility of ions prevents any chance of forming diffuse double layers. Indeed, charged particles suspended in a non-aqueous surrounding will not be “screened” by counter-ions (as they are in electrolytes) and will often be subjected to long range Coulombic interactions.

There is another common type of interactions in non-aqueous systems which involve large molecules or “macromolecules” (Van Der Hoeven and Lyklema 1992, 205-277). Bitumen consists of fairly large and heavy molecules that include aliphatic side chains and polar hetero-atoms; these molecules could behave, to some extent, as macromolecules. When some of these macromolecules adsorb onto the surfaces of suspended solids, inter-particle interactions can be profoundly affected. Indeed, these adsorbed layers can often control the overall stability of a colloidal dispersion. What results from this adsorption depends on

several factors, including the mechanism of macromolecule adsorption on the solid substrate, the relative amounts of macromolecules and solvent, and the method of mixing. In other words, the “quality” of the solvent (using terminology from polymer physics) and the amount of adsorbed macromolecules will determine if the overall particle-particle interaction is repulsive (steric repulsion) or attractive (molecular cross-bridging) (Butt, Graf, and Kappl 2003).

### **2.2.2.1 Steric Repulsion**

Many colloidal dispersions are stabilized by the adsorption of macromolecules onto the particle surfaces; the stabilization is due to an underlying interaction called the steric repulsive force. In “good solvents,” macromolecules adsorbed on the surface tend to extend into the solvent and form tails and loops. Having macromolecules closely packed on the surface, tails and loops will contribute to an elongated “brush” shaped structure. In this case, when two particles with covered surfaces approach one another very closely, it will cause the brushes to repel each other, thus leading to a short-range steric repulsion between the particles (Butt, Graf, and Kappl 2003). By substituting the good solvent with a bad one, the molecular brush will be more flattened onto the surface and no more steric repulsion would be sensible. A schematic of this phenomenon is shown in Figure 2.4.



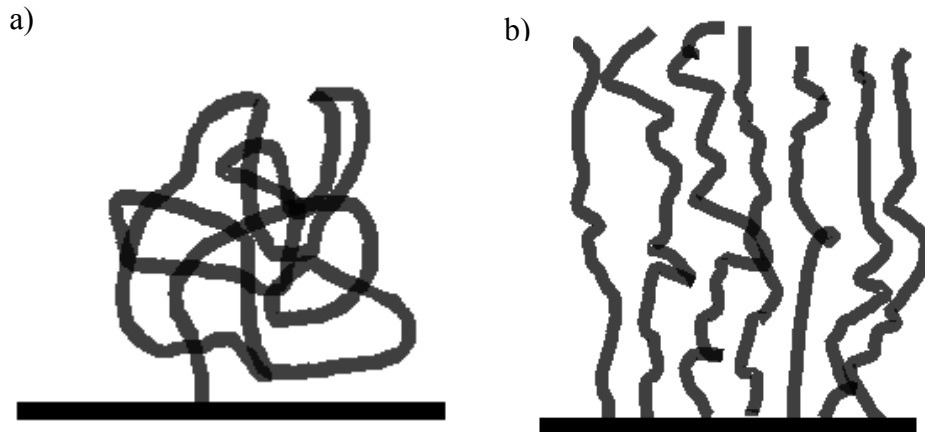


Figure 2.4: Macromolecules adsorption on the surface in a) bad solvent (packed structure)  
 b) good solvent (brush-like structure)

### 2.2.2.2 Cross Bridging

Although the existence of macromolecules in colloidal suspensions can lead to steric repulsive forces, it is not always the case. Sometimes it can appear in the form of an attractive force, resulting in destabilization and flocculation. When macromolecules are sparsely adsorbed onto suspended particles, and if they are long and flexible enough, they may latch onto two adjacent particles, resulting in a cross-bridging phenomenon (Figure 2.5). This occurs at particle separations that are comparable to the size of the macromolecule (Butt, Graf, and Kappl 2003). (Note that the “size” of the macromolecule is a function of its conformation, which in turn depends on the “quality” of the surrounding solvent.). Thus, in the light of cross-bridging mechanism, macromolecules can function as flocculants which help to precipitate colloids.

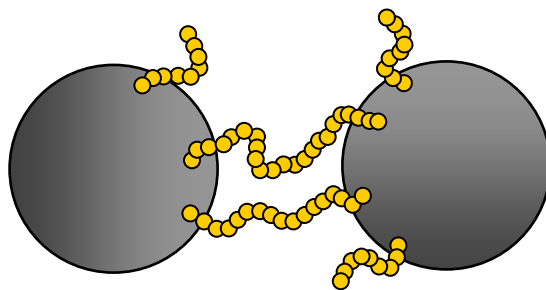


Figure 2.5: Polymer cross-bridging between two particles

### 2.2.3 Inter-Particle Force Measurement Methods

Behaviour of colloidal suspensions depends on the superposition of all different types of forces. Here, the two most common methods for measuring inter-particles forces are described. In addition, a novel micro-cantilever technique, which is an in-house developed method, is introduced briefly. A more detailed description of this new method will be given in Chapter 3.

#### 2.2.3.1 Surface Forces Apparatus

The surface forces apparatus (SFA) is an instrument that can directly measure forces occurring between two curved surfaces in liquid and vapour media with angstrom resolution (Israelachvili and Adams 1978, 975). The surfaces are two crossed cylinders covered with molecularly-smooth mica sheets (Figure 2.6). One of these cylindrical surfaces is connected to a piezoelectric translator which adjusts the separation distance between the surfaces. The other mica surface is mounted onto a deflectable spring with a known spring constant. The separation of the two cylinders can be measured by use of an optical technique, with resolution of one angstrom. The deflection of the spring can be calculated by knowing the position of one cylinder and its distance from the second cylinder

surface. Applying Hooke's law, multiplying spring constant by deflection, the force can be calculated (Butt, Graf, and Kappl 2003)(Israelachvili and Adams 1978, 975-1001).

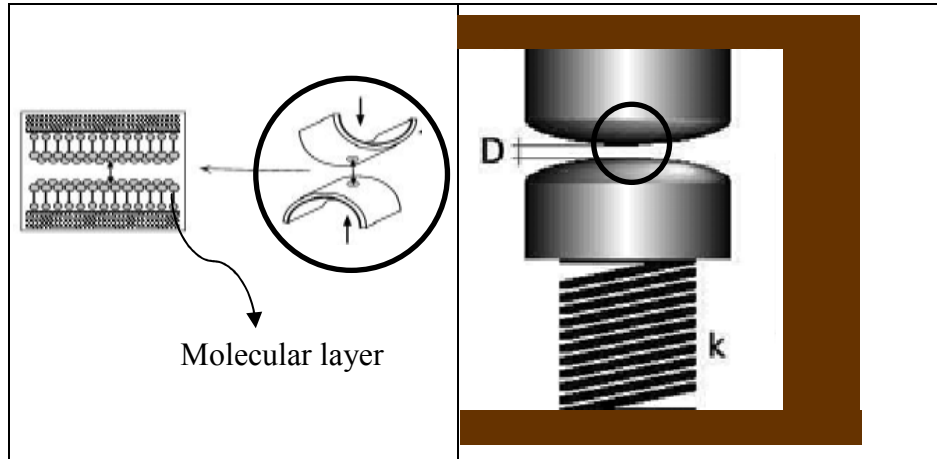


Figure 2.6: Schematic of a surface force apparatus (SFA) and its two crossed mica cylinders.

### 2.2.3.2 Atomic Force Microscope

The atomic force microscope (AFM) is another direct surface force measurement technique; it is a member of a family of techniques known as “scanning probe microscopy.” Applying this device, the colloidal force between a planar surface and an individual colloid particle can be measured in a liquid or a vapour. To do so, a spherical colloid particle (approx. 10  $\mu\text{m}$  in diameter) is fixed on the tip of an AFM cantilever. This cantilever is positioned over a sample surface and is used to scan the specimen surface; the entire assembly can be immersed in a liquid. When the tip is brought into close proximity of a sample surface, forces between the tip and the sample result in deflection of the cantilever. This deflection is detected by shining a laser beam onto the back of the cantilever, which is reflected off the back surface and ends up on a position

sensitive detector (PSD); the PSD produces an output signal which is proportional to the deflection of the cantilever (Figure 2.7). Employing again Hooke's law, the surface forces can be determined as a function of separation distance (Butt, Graf, and Kappl 2003).

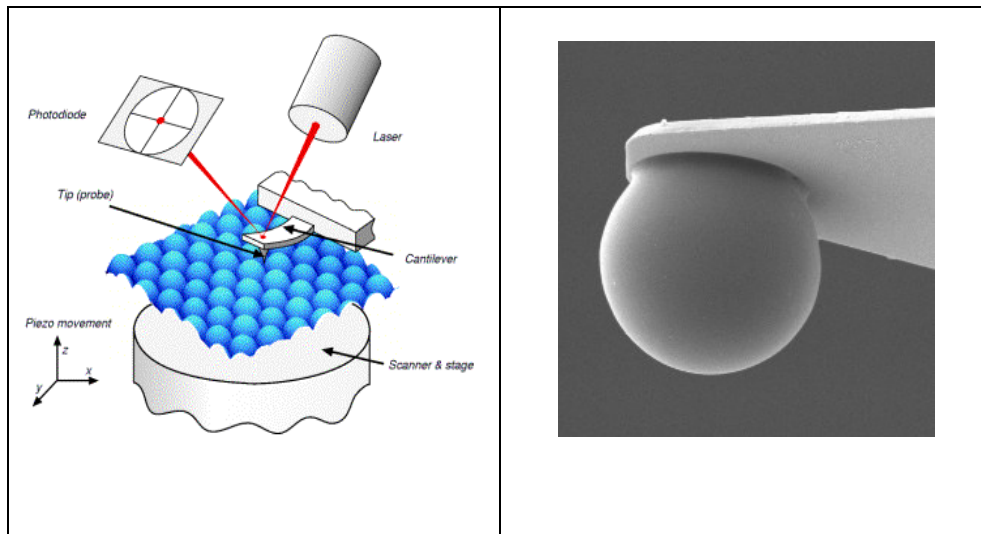


Figure 2.7: Schematic of an atomic force microscope (left) and an example of colloidal probe (right). The picture shows a glass sphere with a diameter of approximately  $10\ \mu\text{m}$  that is glued to the end of a triangular AFM cantilever.

As mentioned, the SFA and AFM both can be used for force measurement purposes in liquid media. When it narrows down to non-aqueous media, most of the work has been done by SFA, and there is not any noticeable force measurement results in oil media using the AFM. It seems the lack of work in this area may be related to the fact that the liquid cell of AFM is not particularly suited for non-aqueous environments (Wang et al. 2009, 862-869). One ubiquitous component of our experiments is toluene, which is particularly harsh on AFM cells due to its tendency to cause leaching of contaminants from solid surfaces. To avoid any contamination, the new micro-cantilever technique was developed in our laboratory to suit our experimental needs.

### **2.2.3.3 Microcantilever Technique**

In what follows, a novel micromechanical technique is introduced which is capable of measuring inter-particle forces (Moran, Yeung, and Masliyah 1999, 8497-8504)). In this method, the tips of a glass micropipette and glass microcantilever function as solid particles (note that the surface properties of glass can be modified through various chemical means). Under a microscope, the rounded glass tip of the micropipette is manipulated into contact with the tip of the microcantilever, which is mounted and fixed. The entire system is surrounded by a third phase, which in our case is a hydrocarbon. Once the tips are in contact, the micropipette is pulled back. If there is any adhesive force between the glass particles, the cantilever tip will be attracted to the micropipette tip and would deflect from its original position. The cantilever movements are recorded during the experiment.

The force measurement experiments are observed with an optical microscope connected to a camera and a computer. The video sequences are recorded with a software for cantilever deflection measurements. A sample image of such an experimental setup is seen in Figure 3.7. Knowing the cantilever stiffness and also its deflection during the experiment, one can easily deduce the adhesive force using Hooke's law. A more detailed description of the micro-cantilever method will be given in Chapter 3.

### **3 Materials and Methods**

The flocculation of silica particles in hydrocarbon media will first be studied on the macro-scale, then followed by micro-scale experiments. In macro-scale experiments, the settling rate of micron-sized silica particles in different hydrocarbon media (some of which containing bitumen) is measured. On the micro-scale, we developed a novel micro-cantilever technique to determine the inter-particle forces between glass surfaces in hydrocarbon environments.

#### **3.1 Macro-Scale Experiments: Settling tests**

##### **3.1.1 Materials**

###### **3.1.1.1 Solid Particles (the dispersed phase)**

In this study, 0.25- $\mu\text{m}$  silica particles (Fiber Optic Center Inc.) were surface-modified in two different ways, resulting in what we will call “clean” and “bitumen-coated” particles.

###### *Clean silica*

To prepare clean silica particles for our experiments, the factory received beads were heated in a muffle furnace (Thermoscientific Thermolyne heavy duty muffle furnace, model FA1730) at 650°C for 2 hours to remove any possible chemical residue on the surface.

###### *Bitumen-coated silica*

For bitumen-coated spheres, our goal was to leave a layer of irreversibly adsorbed bitumen material on the particle surfaces. To achieve this, the following procedures were followed: We first prepared a toluene-diluted bitumen solution at 1:4 ratio (i.e. one part bitumen to 4 parts toluene by weight). The bitumen was the so-called ‘vacuum topped’ sample provided by Syncrude Canada Ltd. The toluene was HPLC grade from Fisher Scientific; it was used as received without further purification. Next, clean silica beads were dispersed in toluene-diluted bitumen at 4 wt% (e.g. 4 g of clean silica in 100 g of diluted bitumen solution). To ensure that all the silica particles were evenly wetted (i.e. no dry clumps in the suspension), 10 mL of the diluted bitumen solution was first added to the silica powder to make a paste. After 10 minutes of mixing, the remaining of the solution was added. To avoid attachment of wet silica particles to the container walls, Teflon bottles (NALGENE Labware, FEP material) were used for all preparation steps. The suspension was then agitated by a magnetic stirrer (VWR Scientific Products) for 30 minutes to allow adsorption of bituminous material onto the silica particle surfaces. After this, the silica beads were washed multiple times with fresh toluene using a centrifuge (Beckman, model JA-10) as follows: The suspension was centrifuged for 15 minutes at 4000 rpm until the supernatant was free of solids. The supernatant was then discarded and replaced with clean toluene, and the new suspension was vigorously agitated. This was repeated until the supernatant appeared clear (i.e. free of any bitumen). The reason for multiple washing was to ensure that the only remaining bitumen was the irreversibly adsorbed layer of bitumen material on the particle surface which could not be

washed off with toluene. At the end, the bitumen-treated solids were recovered by pouring the supernatant out and drying the solids under a fume hood for 2 days. Finally, the slightly blackened powder, which was our bitumen-treated silica particles, was collected in a glass bottle and ready for experimentation. Silica particles that have undergone this special type of surface treatment are assumed to closely mimic the indigenous fine particles in oil sand ores, i.e. particles that have been in contact with bitumen for extended periods of time.

#### **3.1.1.2 Hydrocarbon (the continuous phase)**

To investigate the aggregation behavior of silica particles in hydrocarbon (similar to what occurs in paraffinic froth treatment), toluene and *n*-heptane (both HPLC grade, purchased from Fisher Scientific) were used as the solvents. For our preliminary experiments, the hydrocarbon media were pure solvents of variable toluene-to-heptane ratios. As the experiments went further, bitumen with different mass ratios (5 wt% and 10 wt%) were also introduced to the system. This diluted bitumen solution served as a more realistic approximation to the hydrocarbon encountered in an actual froth treatment operation.

#### **3.1.2 Sample Preparation for Settling Tests**

To study the settling behavior of silica particles (clean or bitumen-treated) in a hydrocarbon environment, a solvent consisting of different volume ratios of heptane to toluene (the so-called ‘heptol’ mixture) was used in our experiments. A heptol solution was specified by its *toluene content* in volume percentage; it ranged from 0% (i.e. pure *n*-heptane) to 100% (i.e. pure toluene). To extend our



studies to more realistic oil phases, bitumen may also be added to the heptol solution in some experiments. The amount of bitumen in the oil phase was 0 wt% (i.e. only heptol), 5 wt%, or 10 wt%. After preparation of the hydrocarbon solution, silica particles (either clean or bitumen-coated) were added to the liquid at 1 wt% solids content. The suspension was contained in a teflon bottle and agitated in a water bath sonicator (Transonic 310) for 5 minutes to ensure adequate mixing.

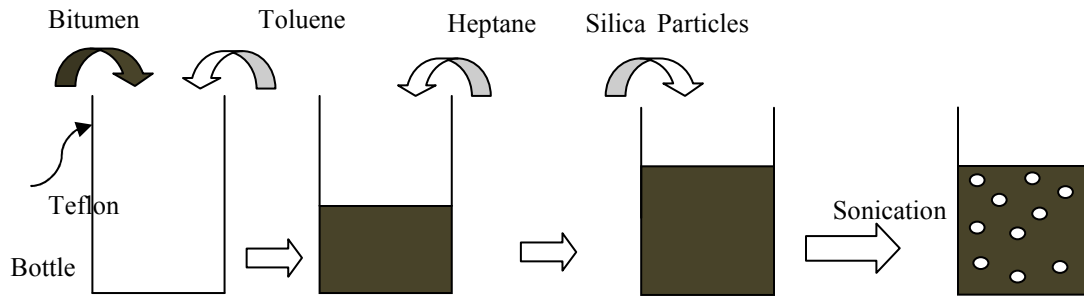


Figure 3.1: Sample preparation procedure

### 3.1.3 Settling Rate Measurement

In this study, the particle settling rate was used as an indicator of how fast the fine solids could form flocs and settle to the bottom of the test bottle. The objective here was to understand the relation between the solids settling rate and the type of hydrocarbon solvent that was involved.

In this study, we introduced a new method of quantifying settling rates by tracking the solids content at a *fixed* location over time. This is a more suitable approach than the common method of following the sludge zone interface (i.e. the

interface between the top clear liquid and the sludge). The traditional method, which is based on optical detection of the sludge zone interface, was not applicable here because of the opacity of the solution wherever bitumen was present in the system. Our new method of quantifying settling rates proceeded as follows:

As mentioned above, a suspension of evenly dispersed particles in hydrocarbon was created after 5 minutes of sonication. The time  $t = 0$  was defined as the moment when sonication ceased and the solids were allowed to settle under gravity. As the particles flocculated and settled, the solids content at any fixed location — assuming it is near the top of the suspension — would diminish over time. Considering this fact, 0.5 mL samples were taken at different times (beginning at  $t = 0$ ) from a location that was along the centre line of the bottle and always 1 cm from the free surface of suspension; these small volumes of suspension were placed in individual crucibles. The sampling volume of 0.5 mL, and the sampling location of 1 cm, were chosen rather arbitrarily (These parameters, however, must be kept fixed to ensure consistency of experimental protocol). A sketch of this procedure is shown in Figure 3.2.a.

To determine the solids contents in the 0.5-mL samples, the small volumes in the crucibles were first placed under a fume hood for an hour to allow the solvent to evaporate. The samples were then transferred to a muffle furnace (at  $650^{\circ}\text{C}$ ) and left for 30 minutes to ensure all but the inorganic materials (in this case, the silica beads) were vaporized. After this ‘ashing’ process, the amount of silica

could easily be determined by weighing the crucibles on a sensitive microbalance (Mettler Toledo, model MX5). As such, we could obtain accurate measures of the solids content at a fixed location (in our case, 1 cm from the free surface) over time. A typical plot of the solids mass  $m$  vs time  $t$  is shown in Figure 3.2.b. In this study, the initial slope of the  $m$  vs  $t$  plot was taken as a measure of the solids settling rate (Figure 3.2.b).

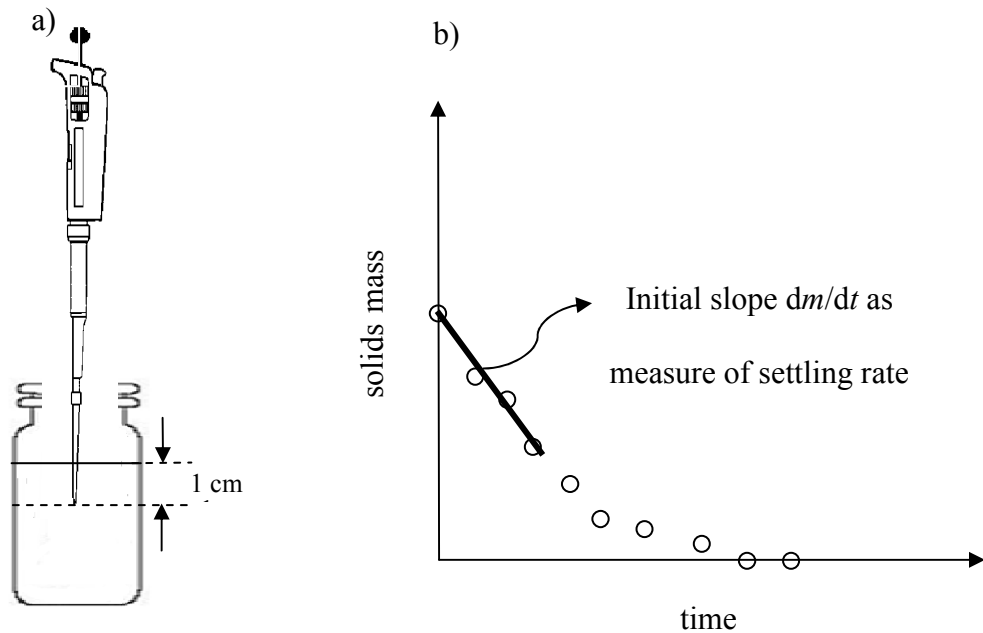


Figure 3.2 : Schematic of the sedimentation experiment. (a) Samples were taken from a fixed location — in this case, 1 cm from the free surface. The amount of solids in each sample was denoted  $m$ , and the settling time denoted  $t$ . (b) Typical plot of  $m$  versus  $t$ .

The initial slope  $dm/dt$  was chosen as a measure of the settling rate.

With this approach, different types of solids and hydrocarbon media were tested for their settling behaviours. The various systems that were studied are listed below in Table 3.1.

Table 3.1: Solids and the corresponding hydrocarbon phases that were studied.

<b>Solid (silica) particles</b>	<b>Oil phase</b>
Bitumen-treated silica particles	Pure solvent (heptol)
Clean silica particles	5 wt% bitumen in heptol
Bitumen-treated silica particles	
Bitumen-treated silica particles	10 wt% bitumen in heptol

### **3.2 Micro-Scale Experiments: Inter-Particle Force Measurements**

In this study, a novel *micro-cantilever* technique was used to quantify the inter-particle adhesive forces between micron-sized glass spheres in non-aqueous surroundings. Details of this micro-scale technique are discussed below.

#### **3.2.1 Materials**

##### **Preparation of Solids Free Toluene-Diluted Bitumen**

In this set of experiments, solids free bitumen was required for treating the micron-scale glass sphere surfaces (these glass spheres were in fact the tips of micropipettes; see section 3.2.2). To ensure a uniform coating of bituminous material on the glass surface, we must first remove all colloidal clay particles from the bitumen, as deposition of these clays onto the glass substrates would interfere with force measurements. To remove the clays, 45 g of bitumen was diluted by toluene at a 1:1 mass ratio. The diluted bitumen solution was then centrifuged at 20,000 g (Thermo Electron Corporation, model RC 6 Plus) for 75

minutes (Gu et al. 2002, 1859-1869). The minimum size of the particles that could be eliminated by centrifugation can be estimated using the Stokes equation:

$$V_s = \frac{d^2 g (\rho_p - \rho_f)}{18 \mu} \quad (3.1)$$

Here,  $V_s$  (m/s) is the particle settling velocity,  $d$  (m) is the hydrodynamic diameter of the particle,  $g$  (m/s<sup>2</sup>) is the gravitational acceleration,  $\rho_p$  (kg/m<sup>3</sup>) is the density of the particles,  $\rho_f$  (kg/m<sup>3</sup>) is the density of the fluid, and  $\mu$  (Pa·s) is the fluid viscosity. The particle settling velocity  $V_s$  can also be expressed in terms of its sedimentation distance:

$$V_s = \frac{l}{t} \quad (3.2)$$

where  $l$  (m) is the length of the centrifugal tube and  $t$  (s) is the centrifugation time.

Substituting equation (3.2) into the Stokes formula (3.1) results in

$$\frac{l}{t} = \frac{d^2 g (\rho_p - \rho_f)}{18 \mu} \quad (3.3)$$

where the particle diameter,  $d$ , is the only unknown. For the remaining variables in the above equation, we assume the following typical values:

- Viscosity of toluene-diluted bitumen:  $\mu = 5.15 \times 10^{-3}$  Pa·s
- Density of toluene-diluted bitumen:  $\rho_f = 926$  kg/m<sup>3</sup>
- Length of the centrifugal tube:  $l = 10.8$  cm
- Density of the solids:  $\rho_p = 2600$  kg/m<sup>3</sup>.

Using these values and equation (3.3), the minimum diameter of the particles that could be separated from diluted bitumen was determined to be 80 nm. The “solids free” supernatant which resulted from this centrifugation process was what we required for treating the glass surfaces.

### 3.2.2 Preparation of Micropipette with Rounded Tip

Micropipette is a tapered glass capillary tube with a closed rounded tip. An SEM image of a micropipette tip is seen in Figure 3.3.

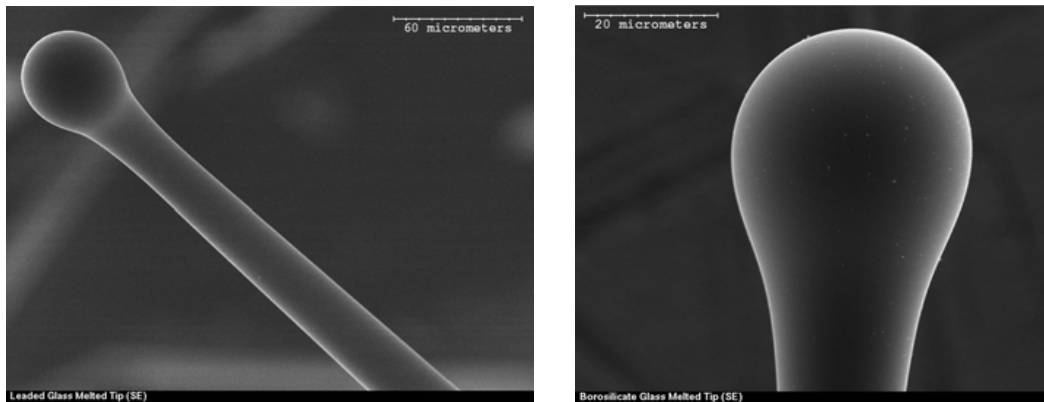


Figure 3.3: Rounded tip of a micropipette

The micropipettes were made from glass capillary tubes with outer diameter 1 mm and inner diameter 0.7 mm (Kimble Glass Inc). To begin, the first step is to taper the capillary tubes. To accomplish this, individual capillary tubes were stretched axially under high temperature using a hot wire pipette puller (David Kopf Instruments, model no. 730), resulting in two separate sections with tapered ends (Figure 3.4). To mimic the characteristics of a single micron sized silica sphere, the tapered end of the glass capillary tube was melted by holding it close to a platinum hot wire (Figure 3.5). The result is a rounded tip micropipette

which could function as silica particles in force measurement experiments. The average diameter of the pipette rounded tip is about 30  $\mu\text{m}$ .

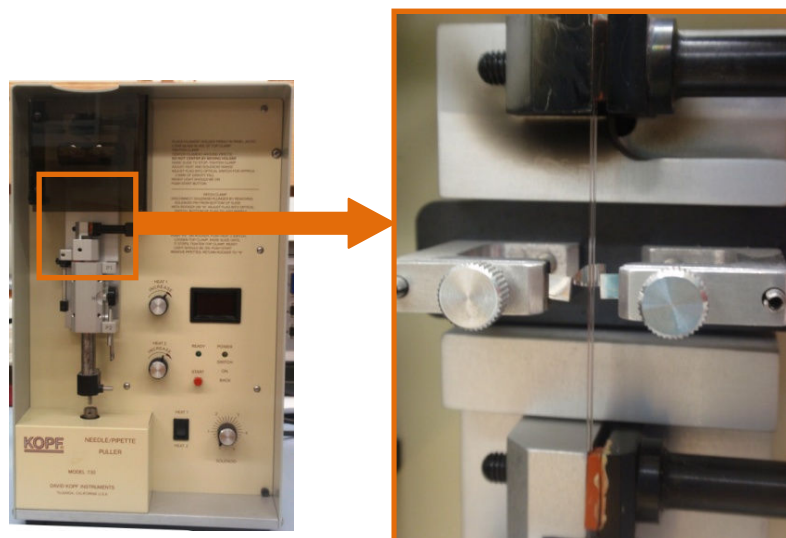


Figure 3.4: Pipette puller apparatus. The magnified picture shows the glass capillary tube (OD: 1 mm and ID: 0.7 mm) positioned in the middle of a platinum wire ready to be stretched at high temperature.

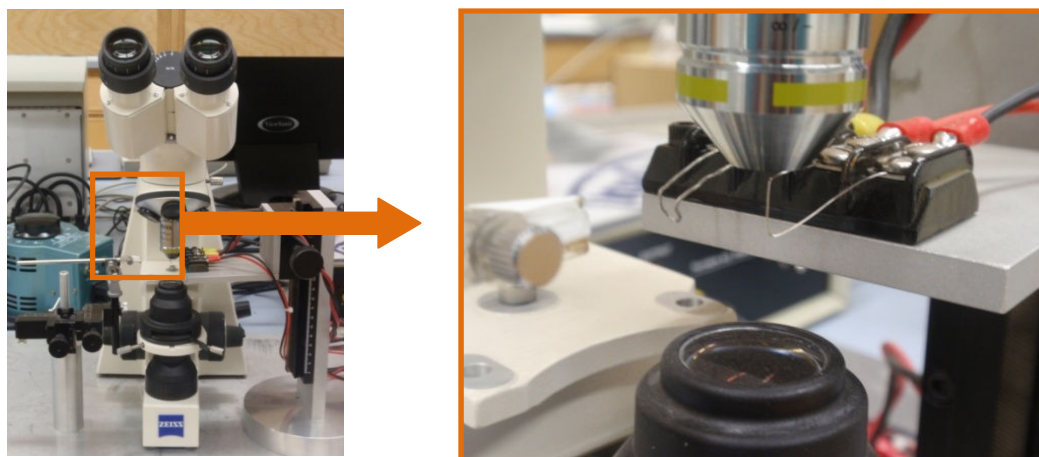


Figure 3.5: The 'micro-forging' apparatus (platinum hot wires shown on the right).

### 3.2.3 Making of the Microcantilever

The microcantilever is a modified type of micropipette that adopts a periscope-like shape, with two right-angle bends as illustrated in Figure 3.6. Such a shape allows for deflection under an external pulling force at its tip, making the device ideal for force detection. The two right-angle bends of the micro-cantilever were created by gently pushing local regions of a straight micropipette against a heated platinum wire; the temperature of the wire was sufficiently high to soften the glass material, but not enough to melt it. The first bend is made very close ( $\approx 100 \mu\text{m}$ ) to the tapered micropipette rounded tip; the second bend is located approximately 5-6 mm from the first bend. During the bending process, care should be given to ensure that the entire microcantilever structure is planar (Moran, Yeung, and Masliyah 1999, 8497-8504).

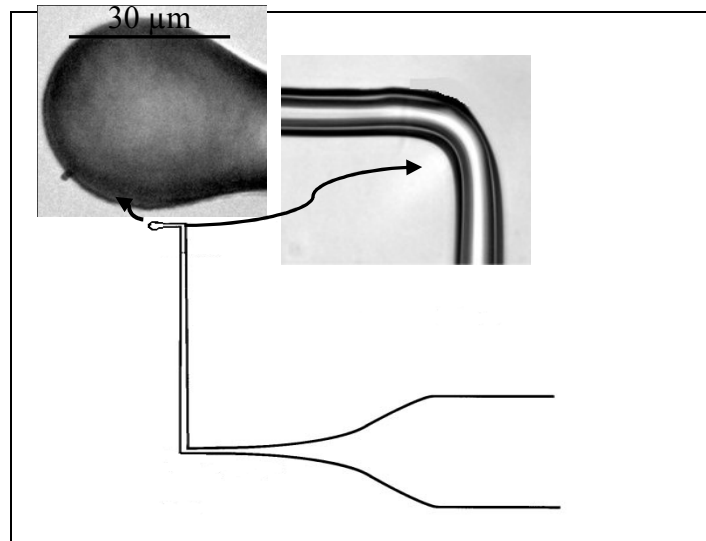


Figure 3.6: A sketch of the micro-cantilever. The magnified views are actual microscope images taken with a 40 $\times$  objective lens. The diameter of the tip is roughly 30  $\mu\text{m}$ .



### 3.2.4 Force Measurements between Two Glass Spheres by the Microcantilever Technique

The microcantilever is a technique for detecting adhesive forces between micron-sized particles; its basic experimental setup is illustrated in Figure 3.7. This method was first developed to study blood cells and biological membranes in the field of biophysics, and has recently been adapted for applications in engineering science and oil sands research (Yeung et al. 2000, 169-181)(Tsamantakis et al. 2005, 176-183)(Yeung et al. 2000, 169-181; Tsamantakis et al. 2005, 176-183; Tsamantakis et al. 2005, 176-183). The procedures for inter-particle force measurement are as follows.

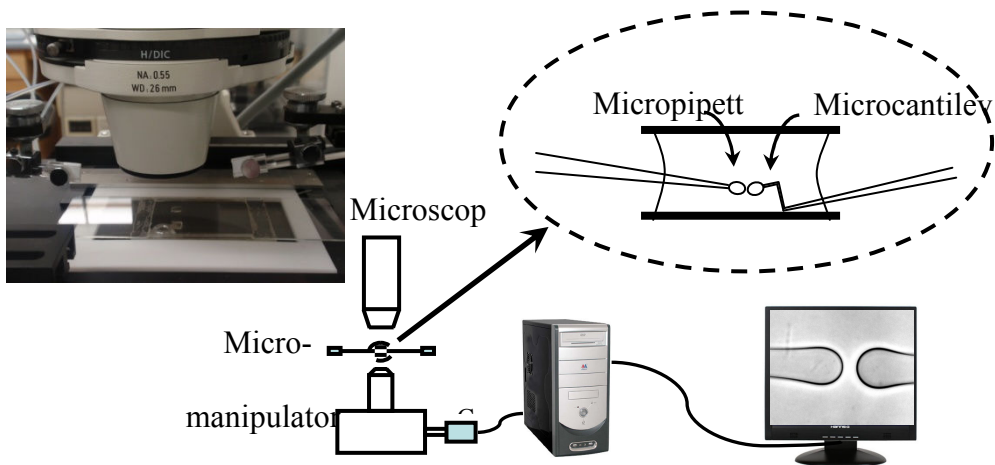


Figure 3.7: A schematic of the micro-cantilever setup. A hydrocarbon solvent was first placed in a small holding cell (also shown in the magnified view). Two micropipettes were then inserted into this environment: a straight pipette from the left, and a micro-cantilever from the right. As seen on the monitor (an actual photograph), both pipette tips had rounded shapes and could function effectively as spherical particles.

For this study, the tips of the micropipette and the micro-cantilever (both rounded in shape and with diameters of roughly 20–30  $\mu\text{m}$ ) will assume the role of glass particles. To begin, the surfaces of these rounded tips were treated with

bitumen — in a manner similar to the treatment of bitumen-coated silica used for the settling tests (see section 3.1.1.1). The tips were first immersed in a solution of diluted bitumen (1:1 ratio, by weight, of solids-free bitumen and toluene) for at least 10 hours; this was to allow sufficient time for the deposition of bitumen material onto the glass surfaces. The tips were then withdrawn from the diluted bitumen solution and thoroughly washed in clean toluene to remove all loose hydrocarbon fragments, leaving only a layer of bitumen material that was irreversibly adsorbed. In this study, we assume the bitumen-treated tips of the micropipette and micro-cantilever (diameters of 20–30  $\mu\text{m}$ ) to have the same surface properties as the bitumen-coated silica (diameter of 0.25  $\mu\text{m}$ ).

For force measurements in this study, the surrounding hydrocarbon medium was solvent-diluted *de-asphalted* bitumen (i.e. bitumen with its asphaltenic components removed; see Section 4.2 for a discussion of the rationale behind using this type of bitumen). As in the settling tests, the solvent used here was a combination of heptane and toluene at various ratios (i.e. heptol). To make de-asphalted bitumen, ‘full’ bitumen was mixed with *n*-heptane at a 40:1 ratio by volume (40 parts heptane + 1 part bitumen). This mixture was then agitated for 2 hours using a magnetic stirrer and allowed to settle for 48 hours. Asphaltene, by definition, is the fraction of bitumen that is insoluble in an aliphatic solvent (here, *n*-heptane). The asphaltenic components will precipitate out as solid residues and settle to the bottom of the container. As such, the supernatant of our heptane + bitumen mixture can be considered asphaltene-free. After evaporation of heptane from the supernatant, what remains will be ‘de-asphalted bitumen.’ This de-

asphalted bitumen will be dissolved in heptol at a concentration of roughly 2 wt%; this will serve as the surrounding hydrocarbon phase for our force-measuring experiments.

After the preliminary preparations, one is now in the position to carry out force measurements. To begin, the hydrocarbon (in this case, heptol-diluted de-asphalted bitumen) is injected into an open glass chamber, which is simply a 1-mm gap between two glass cover slips; the liquid is held in the gap only by capillary forces.

Next, a straight pipette and a micro-cantilever are inserted into the two open sides of the chamber (see Fig 3.7). The rounded tips of these micropipettes, with diameters of typically 30  $\mu\text{m}$ , would function as borosilicate glass particles that interact in a hydrocarbon medium. The two micropipettes are mounted on hydraulic manipulators (Narishige, model MHW-3) which enable smooth 3-D motions of the pipette tips on the micron scale. When positioning the micropipettes, one must ensure that the entire micro-cantilever — including its 5-mm arm — be immersed entirely in the oil phase; this is to avoid any extraneous capillary effects that may interfere with the force measurement. The interaction between the glass tips is monitored using an inverted microscope (Carl Zeiss Canada: Axiovert 200) that utilizes transmission bright-field illumination. The microscope is connected to a CCD camera and a computer. Video sequences of the experiments are recorded digitally so that they can be analyzed at a later time.

With both micropipettes in place, the force-measuring procedures would proceed as follows: We note first that the micro-cantilever is to remain stationary throughout the experiment. Using the hydraulic manipulator, the tip of the straight pipette is brought into contact with that of the cantilever. After gently pushing the two tips together, the straight pipette is slowly pulled back. If the adhesive force between the glass tips is sufficiently strong, the microcantilever will be deflected as the straight pipette is pulled back. With the cantilever behaving as a linear spring, the maximum deflection  $\delta$  of the cantilever tip would be proportional to the adhesive force  $F$ . This maximum deflection  $\delta$  can be easily determined from the recorded video images (see Figure 3.8).

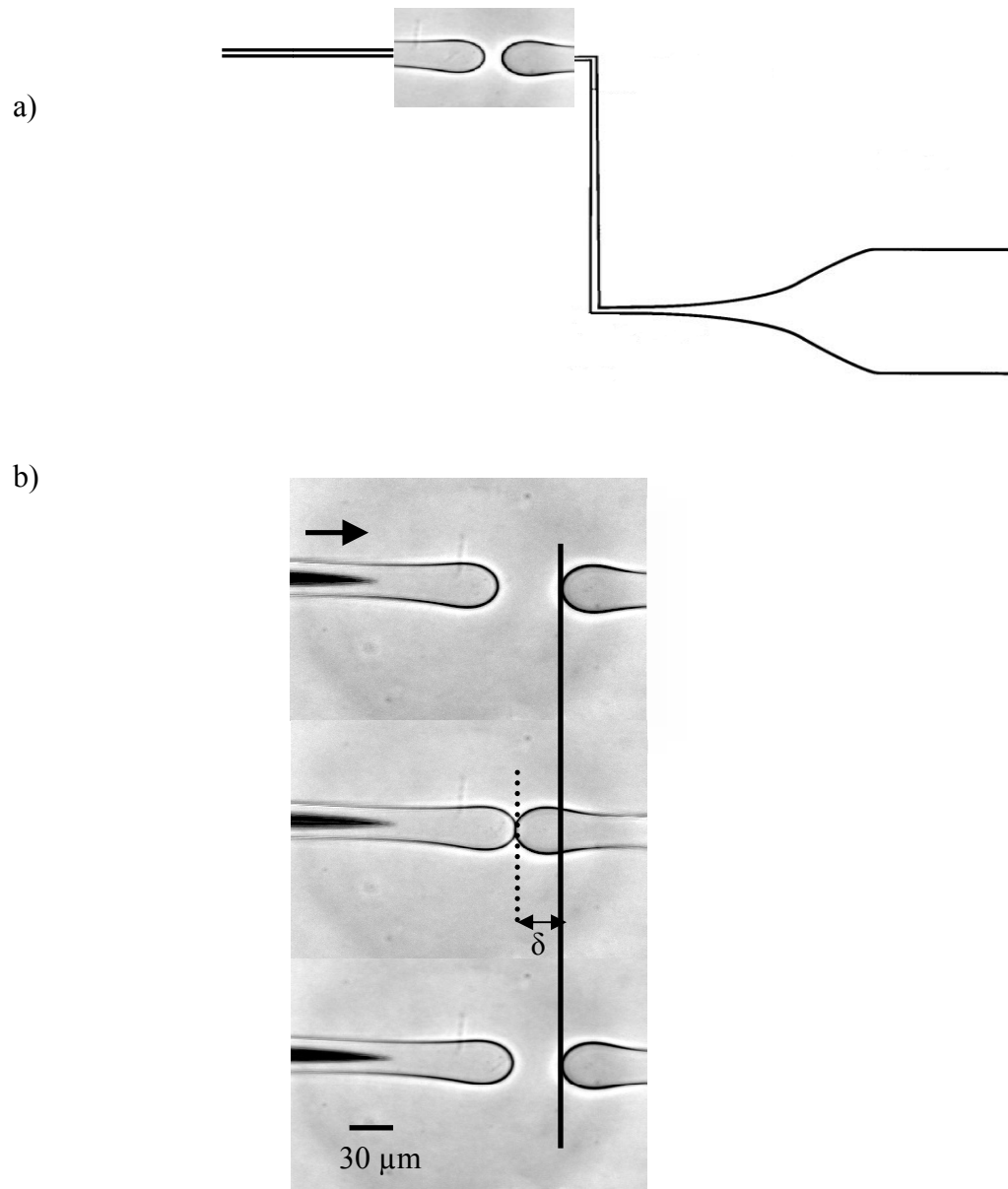


Figure 3.8: (a) A sketch of the microcantilever experiment for determining the adhesive force between two pipette tips (functioning as glass particles). The cantilever on the right was kept stationary throughout the experiment. (b) Actual microscope images of a force-measuring experiment. When the pipette on the left was pulled back, the adhesive force between the tips caused the cantilever to be deflected from its original position by an amount  $\delta$ . The cantilever deflection provides a direct measure of the adhesive force.

To convert the deflection  $\delta$  into a force  $F$ , the effective stiffness of the cantilever  $K_b$  (nN/ $\mu\text{m}$ ) must be known. This stiffness can be calculated straightforwardly from linear beam theory. With knowledge of the Young's modulus of borosilicate glass (approximately  $0.7 \times 10^{11}$  Pa) and the detailed geometry of the 'periscope pipette,' the cantilever stiffness  $K_b$  is obtained from integration of the one-dimensional flexural equation for slender beams. In practice, because every micro-cantilever has its unique shape, the stiffnesses have to be determined individually for each cantilever. Knowing the stiffness  $K_b$  and the maximum deflection  $\delta$ , the corresponding adhesive force  $F$  (nN) between two 'glass spheres' was determined by a Hooke's law-type relation as follows:

$$F = K_b \delta$$

Finally, knowing how to determine adhesive forces, experiments can be done with the same procedures in different types of hydrocarbon environments (i.e. varying toluene contents in the heptol-diluted de-asphalted bitumen).

## 4 Results and Discussion

### 4.1 Macro-scale Experiment: Aggregation of Silica Particles in Non-aqueous Media

We wish to study the sedimentation of fine solids (i.e. silica particles with 0.25  $\mu\text{m}$  in diameter) suspended in a hydrocarbon medium. To begin, the hydrocarbon phase was prepared following the procedure described in section 3.1.1.2. The silica particles were then dispersed in the hydrocarbon through sonication. On the macro-scale, the sedimentation rate of solid particles in heptol (i.e. heptane-toluene mixture) was examined. The independent variable was the aromatic (i.e. toluene) content in heptol, and the dependent variable was the settling rate, which was taken to be the initial slope of the settling curve (i.e. initial  $dm/dt$  of the  $m$  vs  $t$  plots; see Chapter 3).

The reason for the differences in settling rates can be traced ultimately to the inter-particle forces. As discussed in Chapter 2, there are several parameters that can affect these forces and hence the sedimentation rate. These factors include the solid material (and any surface modification that the particles have been subjected to) and the properties of the surrounding media. In this study, we began our experiments with pure solvents (i.e. different volume ratios of *n*-heptane and toluene, but in the absence of bitumen), and developed the work by adding different amounts of bitumen (5 wt % and 10 wt %) to the solvent. Adding bitumen to the suspending medium provides a better simulation of the solvent-based extraction process, as explained in Chapter 1. Moreover, we could

investigate if bitumen introduction to this system would influence the particle settling rates at fixed solids content of 1 wt%.

#### **4.1.1 Effect of Oil Phase Composition on Solids Settling Rate**

The ultimate goal here is to understand — and perhaps control — the settling behaviour of fine solids in diluted bitumen. As discussed in Chapter 1, this has direct relevance to the elimination of unwanted solids in a non-aqueous bitumen extraction process. In this research, the factors that were kept constant throughout all experiments were: the type and size of the primary particles (0.25  $\mu\text{m}$  silica spheres), the way the particle surfaces were treated (exposure to toluene-diluted bitumen), and the solids content (1 wt%). Thus, changes in sedimentation rates result only from alterations in the composition of the suspending liquid. This suspending liquid, which is the oil phase, can be ‘heptol’ (i.e. *n*-heptane + toluene) or heptol + bitumen. Settling results in various oil phases are discussed below.

##### **4.1.1.1 Oil Phase: Heptol (0 wt% bitumen)**

In this set of experiments, a mixture of *n*-heptane and toluene (i.e. heptol) with different volume ratios constitute our oil phase. Here, applying different amounts of toluene and heptane in the solvent medium is a means of varying the aromatic content of the surrounding; it can change from 0 vol% toluene (i.e. pure *n*-heptane) to 100 vol% (i.e. pure toluene). As discussed in Chapter 2, in suspension, the continuous medium’s aromatic content can influence the inter-particle forces and thus sedimentation rate. To begin our study at a preliminary



level, settling tests of bitumen-treated silica in oil phase were first done in a bitumen-free medium (i.e. 0 wt% bitumen). The results are shown in Figure 4.1. In this graph, the horizontal axis represents the amount of *toluene* (in volume percentage) in the heptol mixture; this can be interpreted as the degree of solvent aromatic content. Each data point in Fig. 4.1 shows the settling rate of solid particles (measured by  $dm/dt$ , see Figure 3.2b) in different organic solvents (i.e. different aromatic contents in the heptol mixture). The results show that the settling rate of bitumen-treated silica particles depended strongly on the aromatic content of the solvent: the higher the toluene content (i.e. higher aromaticity), the lower the settling rate. Lower settling rates can be interpreted as increased colloidal stability.

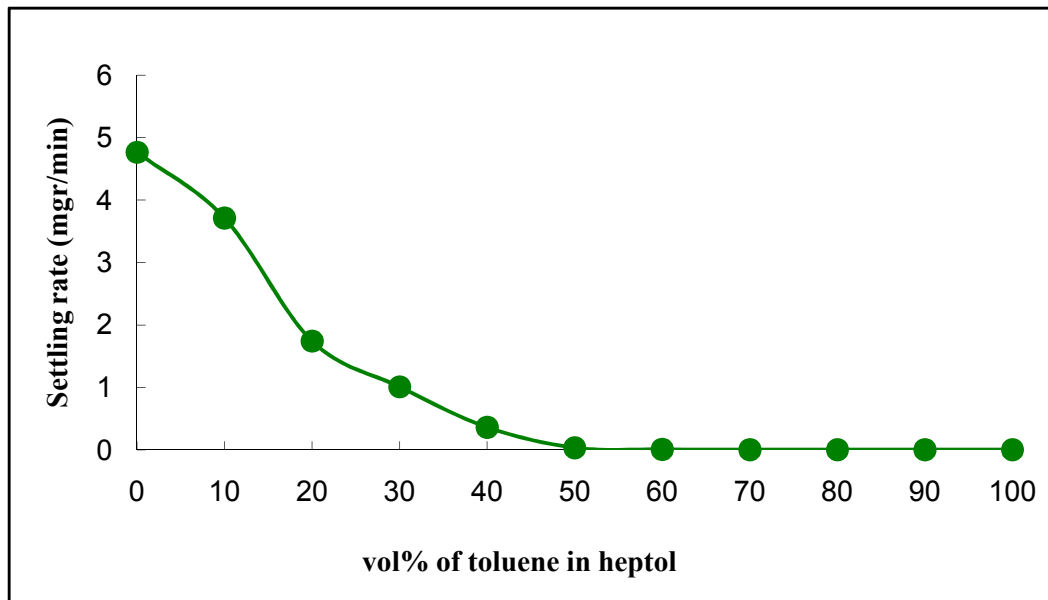


Figure 4.1: Effect of solvent aromatic content on the settling rate of silica particles in heptol (a mixture of toluene and *n*-heptane). There was no dissolved bitumen in the oil phase.

The results in Fig. 4.1 show that for solvents with higher aromatic contents (e.g. >50 vol% toluene), the settling rate is effectively zero. In our experiments, the lowest settling rates, which corresponded to solvents with toluene contents of 60 vol% or higher, were of order  $10^{-3}$  mg/min. Such settling rates, as plotted in Figure 4.1, would appear to be effectively zero. Here, we relate these negligible settling rates to well-dispersed and non-aggregating silica particles (i.e. the silica spheres are colloidally stable in solvents with high toluene contents). On the other hand, the observed non-zero  $dm/dt$  at low toluene contents (i.e. high heptane ratios) could be a consequence of a number of reasons — most notably a broad particle size distribution as a result of flocculation. It follows that any “non-zero”  $dm/dt$  in Figure 4.1 must essentially be due to significant flocculation of the 0.25-micron silica particles.

We speculate that, for solvents containing significant amounts of aromatic (here, toluene) components, the silica particles will repel one another at close range; the reason for this is as follows: due to bitumen treatment of the silica particles, one may assume that asphaltene molecules (i.e. the higher molecular weight components of bitumen) will be anchored to the silica particle surface, forming an irreversibly adsorbed layer. These macromolecules will extend into an aromatic environment (due to its high solvency), forming a “swollen brush” around the particle (see Section 2.2.2.1). As such, when two particles with asphaltene-covered surfaces get close to one another, the adsorbed layers will act as steric barriers which result in a repulsive force (see Figure 4.3b). This steric repulsion is responsible for the overall colloidal stability of the particles in

toluene, and thus very low settling velocities (of order 10  $\mu\text{m/s}$ , according to Stokes law). Therefore, lower settling rates can be expected in solvents with high aromatic contents. Conversely, by substituting the aromatic solvent with one that is paraffinic (e.g. heptane, which is a “bad solvent” for asphaltene molecules), the molecular brushes will shrivel and collapse onto the surfaces (see Figure 4.3a). With the collapse of the steric barriers, the particles are allowed to get close enough to one another for van der Waals attraction to be effective. It follows that aggregates can be formed, which will eventually grow to sizes which settle rapidly. Thus, one could see that higher paraffinic contents of the organic solvent could result in bigger aggregates, which in turn leads to higher settling rates.

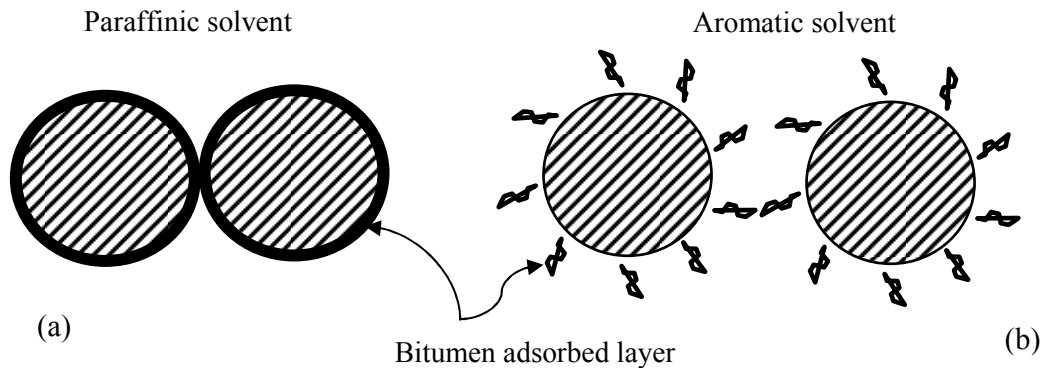


Figure 4.2: Bitumen-coated solid particles in (a) a paraffinic solvent, (b) an aromatic solvent.

Figure 4.3 presents visual confirmation of our assumption about the dependency of settling rate on aggregate size, which itself is related to the aromatic content of the organic solvent. The microscope images are of suspensions of micron-sized *bitumen-treated* silica spheres; the solids content was 1 wt% in all three cases. The silica spheres in Figure 4.3a were suspended in pure

toluene. It appears that no flocs were present under the illumination of optical light (wavelength of approx.  $0.5 \mu\text{m}$ ). Even if flocs were present, it is so small that it cannot be seen. Decreasing the aromaticity of the solvent to 50 vol% toluene and finally to 0 vol% (Figs 4.3 b and c, respectively) appeared to enhance particles homo-flocculation. Referring to this figure, it is obvious that the particles floc size is increasing monotonically with decreasing solvent aromaticity.

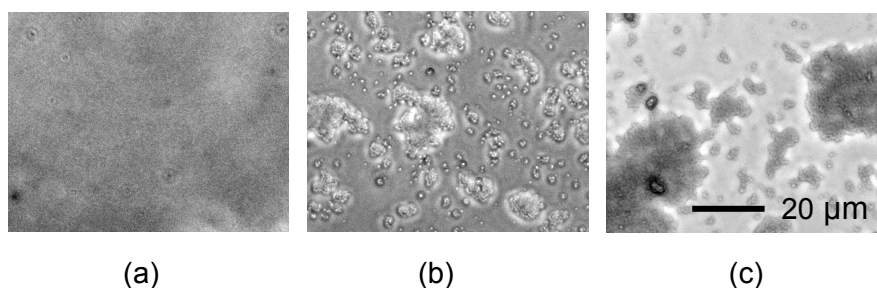


Figure 4.3: Microscope images of bitumen-treated silica in mixtures of toluene and n-heptane at various ratios: (a) 100% toluene, (b) equal volumes of toluene and heptane, (c) 100% heptane.

In addition to this visual confirmation, earlier studies had suggested that the settling behavior of bitumen-coated silica particles in heptol (as an organic solvent) strongly correlated with the nature of the inter-particle forces. Interaction between bitumen-treated surfaces (with main focus on asphaltenes) can be attractive or repulsive, depending on the quality of solvent. We speculate that in the toluene-rich end of the settling rate graph (Figure 4.1), the nature of inter-particle forces is steric (Figure 4.2b). Although there must be some attractive forces as well, it seems that in a good solvent, repulsive forces are dominant. Due to these repulsive forces, one can conclude that the solid suspension is colloiddally

stable. As mentioned in Section 2.2.1, there are different types of adhesive forces between colloidal particles. Most of these forces, however, are not applicable in our non-aqueous environments. We propose that the main attractive forces are due to van der Waals interaction. Depending on the aromaticity of the solvent, van der Waals forces can significantly change. The van der Waals force between two identical spheres can be calculated from Derjaguin's approximation (Butt, Graf, and Kappl 2003):

$$F_{\text{vdW}} = -\frac{R A_{\text{eff}}}{12 D^2} \quad (4.1)$$

where  $R$  is the radius of the sphere (i.e. treated silica particle),  $D$  is the separation distance between two surfaces, and  $A_{\text{eff}}$  is effective Hamakar constant of the system, which, in our experiment is calculated from the expression

$$A_{\text{eff}} = \left( \sqrt{A_{\text{heptol}}} - \sqrt{A_{\text{asphaltene}}} \right)^2 \quad (4.2)$$

The Hamakar constant of heptol is determined by volume averaging, i.e.  $A_{\text{heptol}} = \sum \varphi_i A_{ii}$ , with  $i = T$  for toluene and  $i = H$  for heptane. The quantity  $\varphi_i$  is the volume fraction of component  $i$  in the solvent. The Hamakar constants of toluene and heptane in air had been earlier reported to be  $A_H = 4.5 \times 10^{-20}$  J and  $A_T = 5.4 \times 10^{-20}$  J, respectively (Wang et al. 2010, 183-190). Also, Fotland et al. reported the Hamakar constant of asphaltene in air to be about  $6.0 \times 10^{-20}$  J (Fotland and Askvik 2008, 22-27). Calculating  $A_{\text{heptol}}$  in different aromaticities (by varying the volume ratios of toluene and heptane), and thus  $A_{\text{eff}}$ , shows a

gradual increase of  $A_{\text{eff}}$  with increasing heptane volume ratio. This is consistent with the rising van der Waals forces between particles as more heptane is added, which itself encourages the suspended particles to flocculate by causing the steric layer to collapse. As a consequence, we hypothesize that the nature of inter-particle forces in our experiments is changing from repulsive to attractive as the toluene content in the solvent (heptol) is decreased; this leads to more aggregation and precipitation in heptane-rich heptol. Although this scenario is consistent with our observations, it still remains speculative at this point.

#### **4.1.1.2 Oil Phase: Heptol-Diluted Bitumen (5 and 10 wt% bitumen)**

The simple case of bitumen-treated silica settling in heptol was modified to a more realistic situation: the new oil phase is now heptol-diluted bitumen (the same solid particles, i.e. bitumen-treated silica, were used). The effect of bitumen concentration on the settling rate is shown in Figure 4.4. The solids concentration was kept constant at 1 wt %, and the bitumen concentrations were 5 wt % and 10 wt%. The hydrocarbon phase was composed of heptol (i.e. toluene-heptane mixture at various volume ratios) *and* bitumen. The horizontal axis in Fig. 4.4 represents the volume percentage of toluene in the heptol mixture — before it was used to dilute the bitumen; as such, it is not the overall volume percentage of the oil phase. Each data point in Figure 4.4 is the average settling rate of at least 3 measurements. The results show that the settling rate of silica particles not only changes with the amount of toluene in heptol, but also with the bitumen concentration. More importantly, the settling trend is not the same as in the previous case (see Fig. 4.1), where no bitumen was present in the oil medium.

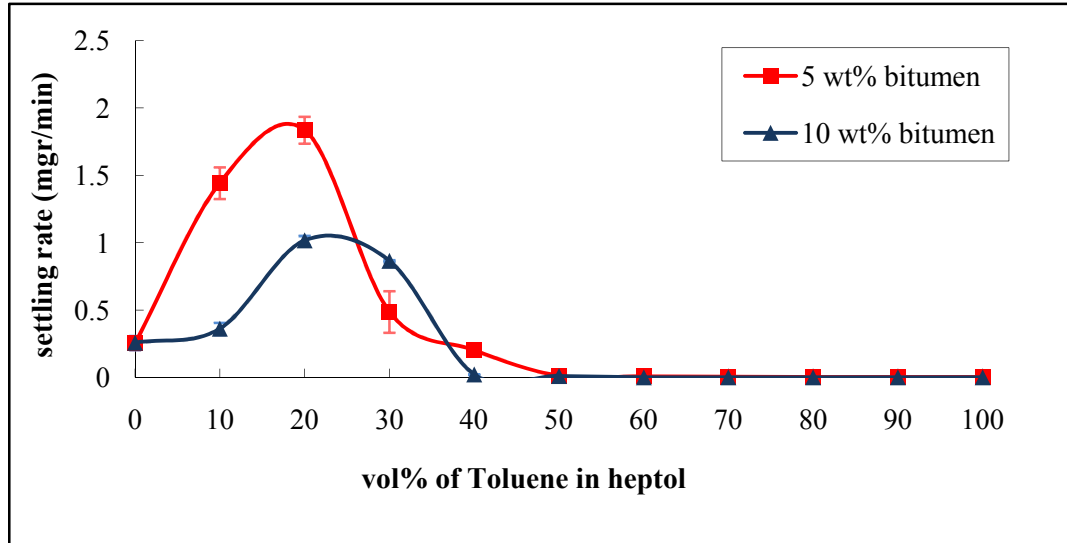


Figure 4.4: Effect of bitumen concentration on the settling rate of bitumen-treated silica. The suspending liquid was heptol-diluted bitumen solution.

Here, the addition of even small amounts of bitumen (e.g. 5 wt%) to the system led to a substantial change in the shape of the settling curve. In comparison with the case of pure solvent as the oil phase (Fig. 4.1), the cases involving diluted bitumen (Fig. 4.4) do not show a monotonic descending trend for the settling rates as the solvent aromaticity was increased. Rather, there appears to be an optimum aromaticity for which the settling rate is maximum. Having a maximum sedimentation rate for the fine solids is clearly of interest to the commercial non-aqueous process (in terms of solids removal from the oil phase). According to the above settling graphs, the settling rate maximum occurred at around 20 vol% toluene. It must be noted that there are two different bitumen-related findings here: The first is that increasing the bitumen content of the oil phase (from 5 wt% to 10 wt%) caused a decrease in the settling rates and sedimentation of silica particles; the other observation is that the nature (i.e. shape) of the settling curve

was changed with incorporation of bitumen into the oil phase — there appears now an optimal settling rate as the aromatic content of the solvent was varied.

Before going any further and suggesting any hypothesis on the mechanism behind these observed behaviors, it is necessary to take a closer look at *asphaltene* as one of the main components of bitumen. Asphaltene is a solubility class of crude oils that precipitate upon dilution by an aliphatic solvent such as *n*-pentane or *n*-heptane; it remains, however, very soluble in aromatic solvents such as toluene and benzene (Long, Dabros, and Hamza 2002, 1945-1952; Long, Dabros, and Hamza 2002, 1945-1952; Long, Dabros, and Hamza 2004, 823-832). In an aliphatic solvent, the asphaltene molecules will precipitate when the ratio of solvent to bitumen exceeds the some onset value. Complete asphaltene precipitation occurs at high ratios of solvent-to-bitumen.

Comparing Figures 4.1 and 4.4, it appears that the values of the settling rate had decreased with introduction of bitumen to the solvent medium. Moreover, increasing the bitumen content from 5 to 10 wt% further decreased the settling rates. Thus, one can conclude that whatever happens in this complex system must be related to the presence of bitumen, specifically the formation of asphaltene precipitates (with addition of different amounts of heptane) and even large networks. Although the homo-flocculation of silica particles is still likely to be a mechanism behind particle sedimentation, the change in settling curve shape (i.e. observation of an optimal point) leads us to consider another parallel mechanism that could justify this kind of behavior for bitumen-involved media.



It has been known that addition of sufficient paraffinic solvent to bituminous material results in asphaltene precipitation. Asphaltene —one of the constituent components of bitumen — is not soluble in paraffinic solvents such as *n*-heptane. It means that once heptane is added to the system, asphaltenes will precipitate, and the precipitated particles tend to flocculate and create flocs or aggregates. These flocs are constantly growing and getting bigger. It was suggested that asphaltene particles with 1  $\mu\text{m}$  diameter could be considered individual primary particles instead of aggregates (Rastegari, Svrcek, and Yarranton 2004, 6861-6870). In cases of bitumen diluted by *n*-alkanes, researchers found that the asphaltene precipitates displayed shape that were far from spherical (fractal-like shapes) with diameters ranging of 80-600  $\mu\text{m}$  (Ferworn, Svrcek, and Mehrotra 1993, 955-959). It is very likely that these big fractal entities of precipitated asphaltene can entrap silica particles (like a fishnet) and cause them to aggregate and settle. If this scenario were true, then the bigger the asphaltene networks, the greater the chances they have of capturing fine solid particles, and hence the more effective is the removal of fine solids. This means having more volume percentage of heptane in our solvent should lead to more asphaltene precipitation, resulting in higher solids settling rates. However, this line of reasoning is in contradiction with our experimental observation, which shows there is a maximum for particle settling rate; in particular, optimal settling appears to be at around 20 vol% toluene — not 0 vol% (as for pure heptane). Our results suggest that although we are expected to observe the biggest asphaltene networks in pure heptane, the highest particle settling rate is not happening for this type of solvent.

Some other mechanisms must therefore be at play in this very complicated process.

Researchers have found that the settling rate of aggregated asphaltenes may depend on many factors, such as the viscosity and density of the solvent medium, and the density and diameter of the asphaltene flocs (Long, Dabros, and Hamza 2002, 1945-1952). A careful examination of these parameters leaves one to speculate that the two important parameters are perhaps the size and density of flocs, and they may explain our experimental results. The other mentioned parameters (density and viscosity of the oil phase) do not change notably between experiments.

Although researchers believe that the biggest asphaltene flocs are observed in cases with pure heptane as solvent (which carries zero aromaticity), it is not clear if they are also the densest flocs. Earlier studies showed that there were two possible mechanisms for floc formation: single particle addition and cluster-cluster aggregation. If single particle addition were the mechanism of floc formation, the produced flocs are more compact and have shapes that are closer to spheres. In contrast, for the alternative cluster-cluster aggregation mechanism, the resulting flocs are usually more open in structure and tend to grow very rapidly. A schematic of these concepts is illustrated in Figure 4.5. It should be noted that producing large flocs (due to the cluster-cluster aggregation mechanism) comes with a significant decrease in floc density, which is not favourable to rapid sedimentation (Gregory and O'Melia 1989, 185).

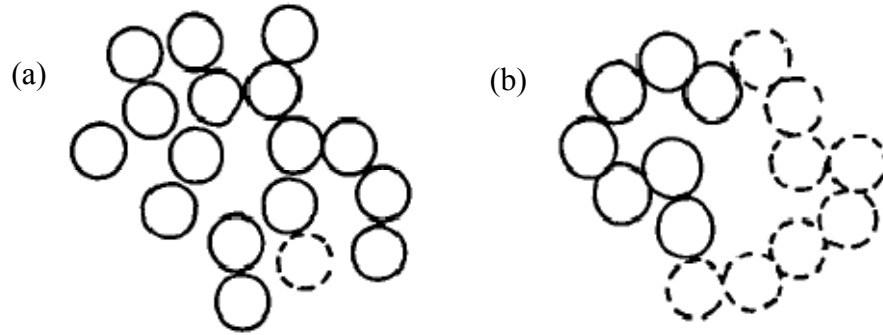


Figure 4.5: Schematic of aggregates formed by (a) single particle addition, and (b) cluster-cluster aggregation.

We postulate that asphaltene flocs formed in heptol with 20 vol% toluene may be denser than those formed in pure heptane, even though the latter situation produces bigger flocs (in other words, asphaltene flocs in pure heptane may be “fluffier” than those in heptol which contains some toluene). Flocs that are denser and with lower porosity will likely settle faster than those that are bigger, but with more “fluffy” structures. Although at this point, we do not have enough experimental facts to support such a conjecture, it could serve as a plausible explanation for such a phenomenon, and will certainly be a fruitful area for future research. A schematic illustration of this hypothesis is shown in Figure 4.6. Still, further study on asphaltene flocculation (how they initially form and grow) is required to understand the mechanism of this process more fully.

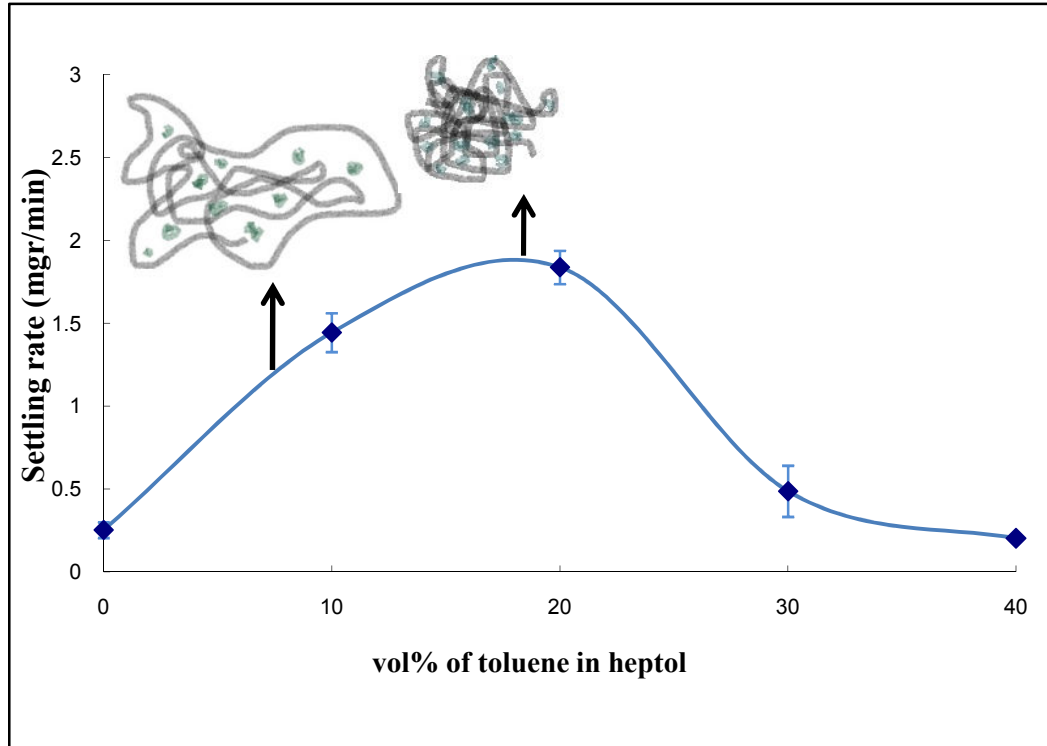


Figure 4.6: Hypothetical schematic of asphaltene floc shapes in heptane-rich heptol. The floc shapes at 20 vol% heptol (i.e. 8 parts heptane + 2 parts toluene by volume) is more spherical and denser than those at higher heptane contents.

Figure 4.4 shows also that, by increasing the bitumen concentration from 5 wt% to 10 wt% (based on the total mass of the mixture), there was a marked reduction in settling rate. That may seem odd at first glance, as more bitumen in the oil phase would imply more asphaltene precipitation — and hence more floc networks to capture and eliminate the solids via sedimentation. There are a number of ways to rationalize this apparent contradiction; one such explanation is as follows: It should be remembered that the bitumen concentrations quoted in Figure 4.4 are based on the *total* mass of the mixture. As such, the higher the bitumen content, the less heptane there is in the mixture to cause asphaltene precipitation — and hence less floc networks to entrap the fine solids. Having

this in mind, it is not hard to envision that more bitumen in the system would lead to less aggregation of the solids, and therefore a slower rate of sedimentation.

#### 4.1.2 Presence of Bitumen Caused a Delay in the Onset of Sedimentation

Compared to the settling of silica in pure solvent (heptol in absence of bitumen), the addition of bitumen to the oil phase had caused an *apparent delay* before sedimentation commenced. Figure 4.7 shows typical  $m$  vs  $t$  curves for 20 vol% heptol; the two curves are for the cases with and without bitumen in the suspending liquid. (The  $m$  vs  $t$  curve, which displays raw data of the settling process, was described in Section 3.1.3.)

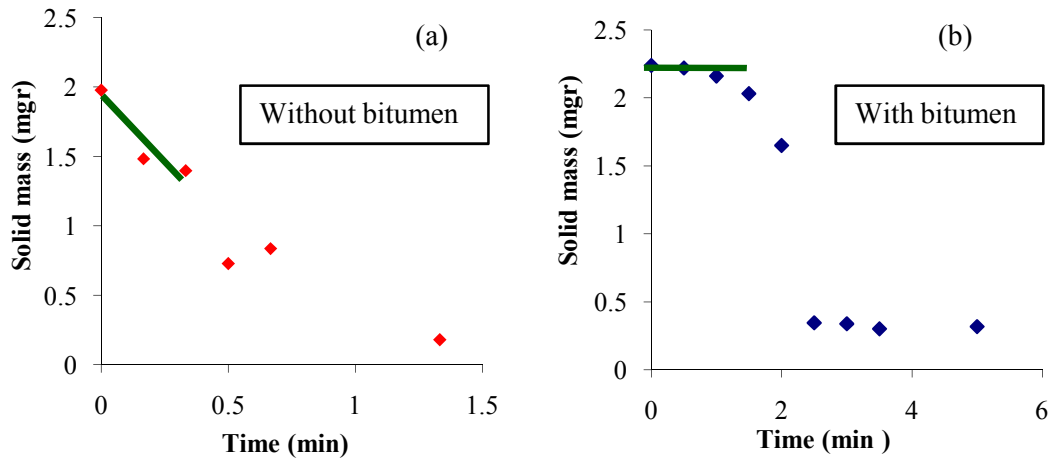


Figure 4.7: Experimental silica particles settling curves for a system (a) without bitumen and (b) with bitumen. In case (a) settling began immediately after mixing was stopped, whereas case (b) shows a *delay time* for particles to begin sedimentation.

Figure 4.7a shows that even right after mixing (i.e. at time  $t = 0$ ), settling was seen to commence immediately. The amount of solids (silica mass after ashing)

in the second sample (taken at  $t = 0.2$  min) was clearly less than the first sample at  $t = 0$ . This shows that the particles began to flocculate and settle immediately after mixing stopped. (Note that Fig. 4.7a exhibits the same characteristics as the imagined  $m$  vs  $t$  curve, as illustrated in Fig. 3.2b.) In contrast, Figure 4.7b shows that for about 2 minutes after  $t = 0$ , no significant change in solids concentration (i.e. the solids mass in 0.5-mL samples) was observed. This implies that, during the initial time interval, very little or no flocculation took place in the suspension. We will refer to this initial period as the *delay time* of the settling process. It should be noted that in our experiments, during the delay period, the concentration of silica particles in the sampling crucibles was around 70% of the initial silica concentration, which suggested fairly well-dispersed suspensions of particles. To study the effect of bitumen concentration on the delay time, Figure 4.8 compares the delay times for two cases of particles sedimentation, with 5 and 10 wt% bitumen content, respectively. The figure also demonstrates the dependence of the delay time on solvent aromaticity. Note from Figure 4.8 that there is no time delay for (i) treated-silica particles in pure heptol (i.e. 0 wt% bitumen), and (ii) when the amount of toluene in heptol was 30 vol% or more.

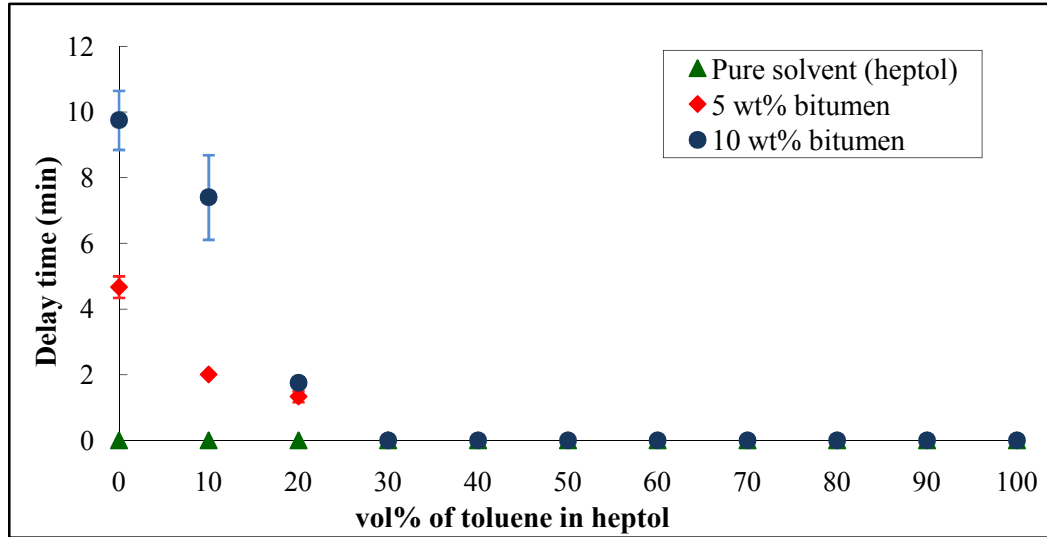


Figure 4.8: Effect of bitumen concentration on the delay time (delay time was illustrated in Fig. 4.7b). Note that the delay time vanished when (i) there was no bitumen in the oil phase, and (ii) the toluene content in heptol was 30 vol% of greater.

These results show that the gradual increase of heptane content in heptol resulted in the sudden appearance of a delay time: starting at 80 vol% heptane (i.e. 20 vol% toluene), the silica particles did not settle immediately, and their tendency of staying in suspension even increased with more heptane. It appears heptane was playing an important role in the observed delay times, provided bitumen was present in the oil phase. It is known that with addition of paraffinic solvents, asphaltene would first precipitate as particles with diameters less than 2  $\mu\text{m}$ , then they flocculate and aggregate into larger entities (Rastegari, Svrcek, and Yarranton 2004, 6861-6870). The key point here is that at the beginning of the precipitation process, it may take some time for the small particles to collide, aggregate, and eventually form floc structures. It appears that, during this time, the silica particles were not flocculating or coming together at all. Indeed, after mixing ceases, the precipitated asphaltene “particles” may inhibit homo-

flocculation of the silica by presenting themselves as steric obstacles. The more heptane was added, the more of these tiny asphaltene particles are released — resulting in more asphaltenic barriers to particle-particle adhesion. This could be the reason for the increase in delay time with heptane content. On the other hand, in the toluene-rich regions of Fig. 4.8, there is no asphaltene precipitation (due to low heptane content) — and hence no time delay before commencement of flocculation.

A more detailed look at these results reveals that, for a given volume ratio of toluene and heptane (i.e. vol% toluene), lower bitumen concentration (e.g. 5 wt% bitumen instead of 10 wt%) resulted in shorter induction times. It is not clear why this was the case. Further investigation into this phenomenon is clearly recommended.

#### **4.2 Micro-scale Experiment: Inter-particle Force Measurements in Non-aqueous Media**

Our goal in this study is to identify conditions under which suspended particulates can be destabilized and settle out. In this regard, the role of inter-particle colloidal forces is clearly of central importance. Thus, to complement the sedimentation studies and provide further insight into the mechanism(s) behind the observed sedimentation phenomena, we also conducted direct measurements of colloidal forces between spherical glass particles (diameters of approx. 30  $\mu\text{m}$ ) in oil media; this was accomplished using the “micro-cantilever” technique. Here,



the rounded tips of the glass pipettes functioned effectively as spherical objects (see Figs. 3.3. and 3.6) on which the colloidal forces acted. This technique involves mounting a micropipette and a micro-cantilever onto the microscope stage, with their rounded tips extended into a chosen oil medium. The tips are then manipulated into close contact, thus allowing the colloidal forces to come into effect. Following close contact of the two rounded tips, the micropipette is pulled back. If there is any adhesive force present, the cantilever tip will be attracted to the micropipette tip, causing the micro-cantilever to deflect from its original position. The cantilever movements are recorded during the experiments. By determining the micro-cantilever deflection  $\delta$  from the microscope images, and knowing the cantilever stiffness  $K_b$ , it is straightforward to calculate the inter-particle adhesive force from Hooke's law, i.e.  $F_{\text{adhesion}} = K_b \delta$  (see also Section 3.2 for a description of this technique).

The glass spheres in this micro-scale study were subjected to the same surface pre-treatment as before (i.e. exposure to toluene-diluted bitumen). The spheres were then made to interact across a hydrocarbon medium. This hydrocarbon medium, however, was slightly different from what was used in the settling tests. For micro-scale force measurements, the experiments were conducted in *heptol-diluted maltene*<sup>†</sup> (instead of heptol-diluted bitumen, which was the oil phase in the

---

<sup>†</sup> In the present context, 'maltene' is *de-asphalted bitumen*. It is the component of bitumen that is *not* asphaltene, i.e. bitumen = asphaltene + maltene. Maltene is by definition soluble in both aliphatic and aromatic solvents.

earlier macro-scale sedimentation study). The reason for choosing diluted maltene as the oil phase is as follows: We wish to understand how the silica particles would aggregate in heptol-diluted bitumen, especially when the solvent is close to pure *n*-heptane (i.e. near 0 vol% toluene). In this regime, the aggregation of fine solids can be due to (a) entrapment of fines by the precipitated asphaltene networks, and/or (b) homo-flocculation of the fines in the surrounding hydrocarbon. As the latter mechanism is largely overlooked by the research community, it is where we shall focus our attention.

In heptane, all asphaltene components in bitumen are precipitated out, leaving the suspending liquid as a diluted maltene solution. Given this scenario, the question we wish to ask is: will the solid particles flocculate with one another in diluted maltene? It is for this question that we will conduct micro-scale adhesion tests in a diluted maltene environment. If the tests came out positive (i.e. if adhesive forces were present in an asphaltene-free medium), then the research community must rethink the mechanism by which solids are destabilized in a paraffinic solvent + bitumen environment: in addition to being caught by the ‘asphaltene nets,’ the solids can also homo-flocculate on their own and settle out under gravity.

In this set of experiments, the surfaces of the glass spheres were bitumen-treated; the hydrocarbon (continuous) phase was heptol-diluted maltene with varying amounts of toluene in the solvent (i.e. in heptol). The maltene concentration was approximately 2 wt% (less than our bitumen concentration in

settling tests) to provide enough visibility under optical light. The results of inter-particle force measurements utilizing the new micro-cantilever method are shown in Figure 4.9.

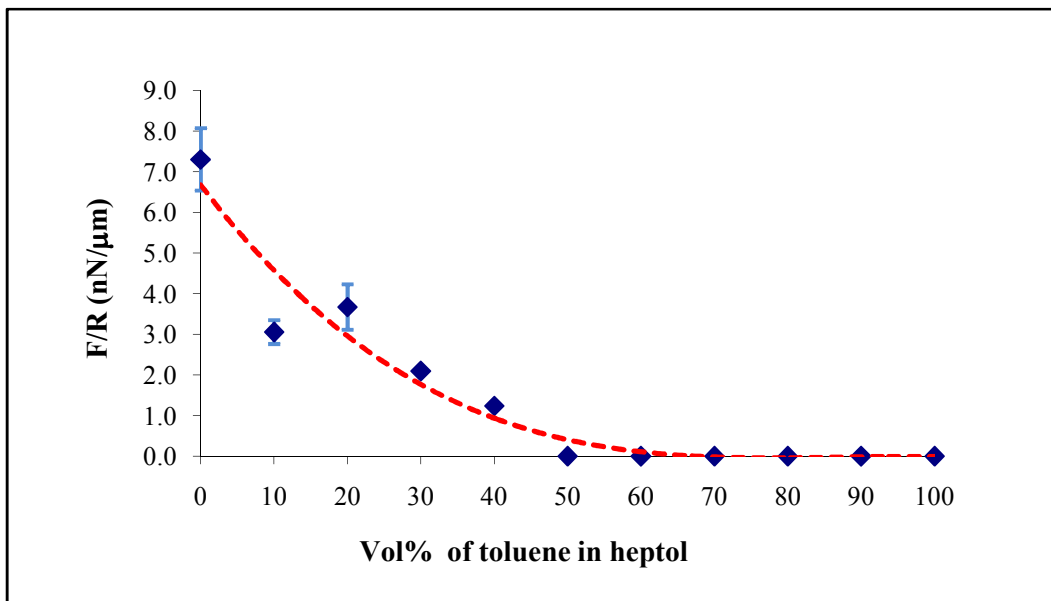


Figure 4.9: Adhesive force between two bitumen-treated glass spheres in heptol-diluted maltene ('maltene' = de-asphalted bitumen). The amount of maltene in solution was approximately 2 wt%.

Here, the horizontal axis represents the toluene content in heptol. Each data point represents the adhesive force between bitumen-treated glass spheres in different aromaticities. Note that the force measurements reported here were scaled by the glass spheres radii (i.e. presented as  $F/R$ , where  $R$  is the radius of curvature of the pipette tip), as is done in many AFM (atomic force microscopy) and SFA (surface force apparatus) studies.

The results in Figure 4.9 show that, in the absence of asphaltene component, the adhesive force between glass spheres is directly related to heptane volume ratio in solvent, and it dramatically increases as the heptane content increases. It

also demonstrates that the absence of such adhesive forces in higher toluene content (i.e. > 60 vol%). This figure can also clarify some of our previous results. In particular, it fortifies our hypothesis on the origin of inter-particle attraction in heptane-rich heptol, and also the absence of such forces in toluene. Previously, we proposed that these adhesive forces were due fundamentally to van der Waals interaction. If the adsorbed layer of bitumen on the silica/glass surface is acting like asphaltene, it will swell and form a brush-like steric barrier in toluene (the ‘good solvent’), thus preventing the particles from flocculating. In contrast, putting the same treated particles in heptane (a bad solvent) will cause the asphaltene layer to collapse onto the surface and hence make it possible for particles to come closer to one another. In this situation, the van der Waals attraction between particles can come into effect (see Fig. 4.2 for a sketch of this proposed scenario). The inter-particle force results in the Figure 4.9 also confirm this hypothesis.

Several conclusions/speculations can be made from the above results:

- The striking similarities between Figure 4.1 (silica particles settling in pure heptol) and Figure 4.9 (glass spheres interacting across diluted maltene) suggest strong correlation between the rate of particle sedimentation on the macro-scale, and the inter-particle forces on the microscopic scale. Moreover, the presence of maltenes in solution is perhaps not interfering appreciably with the van der Waals forces.
- Figure 4.4 represents situations where full bitumen (maltene *and* asphaltene) was dissolved in solution. The shape of this plot is

fundamentally different from those in Figs. 4.1 and 4.9. This suggests that the presence of asphaltene in solution “messes up” the simple trends seen in Figs. 4.1 and 4.9, especially in the heptane-rich regime. The reason is likely due to the presence of small asphaltene precipitates in suspension, which can interfere with the van der Waals interaction by simply “getting in the way.”

- It is long believed that, when a purely aliphatic (i.e. paraffinic) solvent is used to dilute the bitumen, solids removal is due to the asphaltene precipitates forming net-like structures which act to entrap the unwanted solids. Here, we have demonstrated that, even in the absence of asphaltene precipitates, the solids would aggregate (i.e. homo-flocculate) simply through van der Waals attraction. This is clearly seen in Figure 4.9, especially in the heptane-rich regime (left side of the graph).

## 5 Summary and Recommendations

Due to environmental issues accompanied by the current method of oil sands extraction (called the “water-based” extraction), the need for an alternative environment-friendly extraction method is strongly needed. The proposed new extraction approach is called “solvent-based,” which uses no water to liberate bitumen from mined ores. Despite its great benefits, there still are some unsolved issues regarding this method, such as the removal of suspended *fine* particulates from the oil phase (i.e. diluted bitumen) before it enters the upgrading plant. This research is motivated by the above-mentioned obstacle; the intention is to investigate the conditions under which fine solid particles can be separated and removed from the oil medium. The proposed solution in this study was to adjust the solvent “aromaticity” to improve its effects on colloidal solid aggregation in hydrocarbon and thus enhance their settling rates. Here, the settling rate is the observable parameter that directly indicates how a solvent’s aromatic content affects solids removal from the oil phase. As a result, particles settling measurement was the main focus of this study. The settling rate results also provided a better understanding of adhesive forces between micron-sized particles in organic solvents, which could provide more insight into the mechanism behind the paraffinic froth treatment (PFT) process as well.

In this study, micron-sized bitumen-treated silica particles were used to simulate the suspended fines in a real extraction process. The hydrocarbon

medium was composed of different volume ratios of toluene and heptane to allow for different degrees of ‘aromaticity.’

As a preliminary study, the settling of solid particles in pure solvent (with no presence of bitumen except for the particles coatings) was examined. Strong correlation between solids settling rates and solvent aromaticity was observed (see Section 4.1.1.1). These results were then followed by quantitative measurements of solids settling rates for hydrocarbon media containing bitumen.

For hydrocarbon phases that contained bitumen, the particle settling rate measurements indicated there was a strong dependency of settling rates on solvent aromaticity in the presence of bitumen. In contrast to the case of bitumen-free medium, here, the settling results show a maximum rate of sedimentation at a toluene content of approximately 20 vol% in heptol (Section 4.1.1.2). In this set of experiments, in comparison to the former one, the presence of bitumen — most likely its asphaltene fraction — not only changed the values of the settling rates, but also the overall shape of the settling curve. Apparently, asphaltene precipitation plays an important role in entrapping silica particles and forcing them to settle. Moreover, the mechanism of asphaltene precipitation and flocculation are influenced by the solvent’s aromatic content; this could perhaps affect the shape and density of the aggregates, which are crucial to the rate of sedimentation.

Dependency of settling rate on bitumen concentration was also observed. In our experiments, lower bitumen concentration (i.e higher heptane-to-bitumen

ratio) corresponded to higher settling rates. The exact cause for this trend is not clear, but it is likely not due to the negligible changes in viscosity and density of the oil phase. Further investigations are needed.

When bitumen was present in the oil phase, we also observed a ‘delay time’ (of order minutes) which must be past before flocculation/sedimentation commenced. It was found that this delay time only occurred in high heptane-content solvents: higher amounts of heptane resulted in longer delay times. In addition, there appears to be a correlation between bitumen concentration and the delay time.

To provide more insight into the settling of fine solids and its relation to inter-particle forces, a series of micro-scale experiments were conducted. In particular, the *micro-cantilever* technique was used to measure adhesive forces between bitumen-treated glass spheres. In these experiments, the adhesive force between micron-sized glass spheres (which played the role of silica particles in the settling tests) in heptol-diluted maltene was studied. The results showed that, in the absence of asphaltene, there was a strong inverse relation between inter-particle forces and the degree of solvent aromaticity (see Section 4.2). This finding more assured us that the nature of these inter-particle forces to be van der Waals in origin, as we postulated earlier in section 4.1.1.1.

For future work, to study more fully the role of asphaltenes in fine solids removal (from a non-aqueous environment), it is recommended to conduct settling tests in de-asphalted bitumen (i.e. diluted-maltene). Comparing these results with the full-bitumen cases, one can find if the other constituent components of



bitumen also affect the sedimentation of fine particles. If these settling results are in good agreement with our force measurements, it could prove our premise about the nature of the inter-particle interactions. For the same reason, performing force measurement experiments in full bitumen instead of maltenes can be illuminating. Moreover, the kinetics of asphaltene precipitation and flocculation — as vital factors in our solids removal during settling — strongly depends on the properties of the medium and flow conditions such as hydrodynamic shear and temperature. Thus, changing the organic solvent type and also oil phase temperature would be of great interest.

## 6 References

- Anonymous. 2004. Worldwide look at reserves and production. *Oil & Gas Journal* 102, 22-23.
- Board NE. 2006. *Canada's oil sands - opportunities and challenges to 2015: An update. An Energy Market Assessment.*
- Butt, Hans-Jurgen, Graf, Karlheinz, and Kappl, Kappl. 2003. *Physics and Chemistry of Interfaces.* WILEY-VCH Verlag GmbH & Co. KGaA.
- Chia, J., and A. Yeung. 2004. Strength of asphaltene clusters in heptane-diluted bitumen. *Fuel* 83, no. 4-5:619-621.
- Coe, H. S., and Clevenger, G. H. 1916. *Laboratory method for determining the capacities of slime-settling tanks.*
- Farnand, J. R., F. W. Meadus, and B. D. Sparks. 1985. Removal of intractable fine solids from bitumen solutions obtained by solvent extraction of oil sands. *Fuel Processing Technology* 10, no. 2:131-144.
- Ferworn, Kevin A., William Y. Svrcek, and Anil K. Mehrotra. 1993. Measurement of asphaltene particle size distributions in crude oils diluted with n-heptane. *Industrial & Engineering Chemistry Research* 32, no. 5:955-959.
- Fotland, Per, and Kjell M. Askvik. 2008. Determination of Hamaker constants for asphaltenes in a mixture of pentane and benzene. *Colloids and Surfaces A: Physicochemical and Engineering Aspects* 324, no. 1-3:22-27.
- Gregory, J. 1993. The role of colloid interactios in solid-liquid separation. *Water Science and Technology* 27, no. 10:1-17.
- Gregory, John, and Charles R. O'Melia. 1989. Fundamentals of flocculation. *Critical Reviews in Environmental Control* 19, no. 3:185.
- Gu, G., Z. Xu, K. Nandakumar, and J. H. Masliyah. 2002. Influence of water-soluble and water-insoluble natural surface active components on the stability of water-in-toluene-diluted bitumen emulsion. *Fuel* 81, no. 14:1859-1869.
- Homola, A., and A. A. Robertson. 1976. A compression method for measuring forces between colloidal particles. *Journal of colloid and interface science* 54, no. 2:286-297.

- Israelachvili, Jacob N. 1992. *Intermolecular and Surface Forces with Applications to Colloidal and Biological Systems*. 2nd ed. Academic Press.
- Israelachvili, Jacob N., and Gayle E. Adams. 1978. Measurement of forces between two mica surfaces in aqueous electrolyte solutions in the range 0–100 nm. no. 74:975.
- Israelachvili, J. N., and G. E. Adams. 1978. Measurement of forces between two mica surfaces in aqueous electrolyte solutions in the range 0-100 nm. *Journal of the Chemical Society, Faraday Transactions 1: Physical Chemistry in Condensed Phases* 74, 975-1001.
- Long, Yicheng, Tadeusz Dabros, and Hassan Hamza. 2004. Structure of water/solids/asphaltenes aggregates and effect of mixing temperature on settling rate in solvent-diluted bitumen. *Fuel* 83, no. 7-8:823-832.
- Long, Yicheng, Tadeusz Dabros, and Hassan Hamza. 2002. Stability and settling characteristics of solvent-diluted bitumen emulsions. *Fuel* 81, no. 15:1945-1952.
- Moran, K., A. Yeung, and J. Masliyah. 1999. Measuring interfacial tensions of micrometer-sized droplets: A novel micromechanical technique. *Langmuir* 15, no. 24:8497-8504.
- Mossop, G. D. 1980. Geology of the Athabasca oil sands. *Science* 207, no. 4427:145-152.
- Oliver, D. R. 1961. The sedimentation of suspensions of closely-sized spherical particles. *Chemical Engineering Science* 15, no. 3-4:230-242.
- Rastegari, Khashayar, William Y. Svrcek, and Harvey W. Yarranton. 2004. Kinetics of Asphaltene Flocculation. *Industrial & Engineering Chemistry Research* 43, no. 21:6861-6870.
- Richardson, J. F., Harker, J. H., and Backhurst, J. R. 2002. *Coulson and Richardson's Chemical Engineering*. 5th ed. Vol. 2. Elsevier.
- Romanova, U. G., H. W. Yarranton, L. L. Schramm, and W. E. Shelfantook. 2004. Investigation of oil sands froth treatment. *Canadian Journal of Chemical Engineering* 82, no. 4:710-721.
- Sparks, B. D., and F. W. Meadus. 1981. A study of some factors affecting solvent losses in the solvent extraction - spherical agglomeration of oil sands. *Fuel Processing Technology* 4, no. 4:251-264.

- Tsamantakis, Christina, Jacob Masliyah, Anthony Yeung, and Thomas Gentsis. 2005. Investigation of the interfacial properties of water-in-diluted-bitumen emulsions using micropipette techniques. *Journal of colloid and interface science* 284, no. 1:176-183.
- Van Der Hoeven, Ph C., and J. Lyklema. 1992. Electrostatic stabilization in non-aqueous media. *Advances in Colloid and Interface Science* 42, 205-277.
- Wang, Shengqun, et al. 2010. Interaction Forces between Asphaltene Surfaces in Organic Solvents. *Langmuir* 26, no. 1:183-190.
- Wang, Shengqun, et al. 2009. Colloidal Interactions between Asphaltene Surfaces in Toluene. *Energy & Fuels* 23, no. 2:862-869.
- Woynillowicz, D., Severson-Baker, C., and Raynolds, M. 2005. *Oil sands fever: The environmental implications of Canada's oil sands rush*. The Pembina Institute.
- Xu, Y., T. Dabros, and H. Hamza. 2007. Study on the mechanism of foaming from bitumen froth treatment tailings. *Journal of Dispersion Science and Technology* 28, no. 3:413-418.
- Yeung, A., T. Dabros, J. Masliyah, and J. Czarnecki. 2000. Micropipette: a new technique in emulsion research. *Colloids and Surfaces A: Physicochemical and Engineering Aspects* 174, no. 1-2:169-181.
- Zahabi, A., M. R. Gray, J. Czarnecki, and T. Dabros. 2010. Flocculation of silica particles from a model Oil solution: Effect of adsorbed asphaltenes. *Energy and Fuels* 24, no. 6:3616-3623.